The Composition of Dust in Jupiter-Family Comets Inferred From Infrared Spectroscopy

Michael S. Kelley [a,*] and Diane H. Wooden [b]

[a] *Department of Physics, University of Central Florida, 4000 Central Florida Blvd., Orlando, FL 32816-2385, USA*
[b] *NASA Ames Research Center, Space Science Division, MS 245-1, Moffett Field, CA 94035-1000, USA*

Abstract

We review the composition of Jupiter-family comet dust as inferred from infrared spectroscopy. We find that Jupiter-family comets have 10 μm silicate emission features with fluxes roughly 20–25% over the dust continuum (emission strength 1.20–1.25), similar to the weakest silicate features in Oort Cloud comets. We discuss the grain properties that change the silicate emission feature strength (composition, size, and structure/shape), and emphasize that thermal emission from the comet nucleus can have significant influence on the derived silicate emission strength. Recent evidence suggests that porosity is the dominant parameter, although more observations and models of silicates in Jupiter-family comets are needed to determine if a consistent set of grain parameters can explain their weak silicate emission features. Models of 8 m telescope and *Spitzer Space Telescope* observations have shown that Jupiter-family comets have crystalline silicates with abundances similar to or less than those found in Oort Cloud comets, although the crystalline silicate mineralogy of comets 9P/Tempel and C/1995 O1 (Hale-Bopp) differ from each other in Mg and Fe content. The heterogeneity of comet nuclei can also be assessed with mid-infrared spectroscopy, and we review the evidence for heterogeneous dust properties in the nucleus of comet 9P/Tempel. Models of dust formation, mixing in the solar nebula, and comet formation must be able to explain the observed range of Mg and Fe content and the heterogeneity of comet 9P/Tempel, although more work is needed in order to understand to what extent do comets 9P/Tempel and Hale-Bopp represent comets as a whole.

Key words: Comets, Spectra: Infrared, Comets: Dust
PACS: 96.30.Cw, 33.20.Ea

1. Introduction

The dust in Jupiter-family comets (JFCs) is considered to be pristine, that is, little or no processing of the dust has occurred since incorporation into the comet nucleus. We do not equate pristine dust with pre-solar dust. The presence of crystalline silicates in the dust comae of JFCs and Oort Cloud (OC) comets, and the absence of crystalline silicates in the interstellar medium ($\leq$ 2.2%; Kemper et al., 2004, 2005), strongly suggests that much of the dust in comets has been thermally processed ($T \gtrapprox 1000$ K). Strong radiogenic heating may occur in comets of sufficiently large (radius, R_n, > 10–20 km) porous and dust rich nuclei (Prialnik and Podolak, 1999; Prialnik et al., 2008; Merk and Prialnik, 2006; McKinnon et al., 2008), but the presence of highly volatile molecules, such as CO and/or CO_2 observed in the comae of 9P/Tempel (A'Hearn et al., 2005), 21P/Giacobini-Zinner (Mumma et al., 2000), and 103P/Hartley (Crovisier et al., 2000), suggests that comet interiors formed at very low temperatures (as low as ≈ 30 K for CO to condense) and have since remained cold (Yamamoto, 1985; Crovisier, 2007). The simultaneous presence of low-temperature and high-temperature solar nebula condensates in comet nuclei is possible if thermally processed dust can be mixed from the hot inner-solar nebula into the cold comet forming zone (heliocentric distance, r_h, $\gtrapprox 4$ AU) perhaps by turbulent diffusion (Wehrstedt, 2003; Wehrstedt and Gail, 2003, 2008; Wooden et al., 2007) or by large-scale radial (meridional) flows (Keller and Gail, 2004; Ciesla, 2007; Tscharnuter and Gail, 2007).

Mid-infrared (mid-IR) spectroscopy ($\lambda \sim 10$ μm) is an effective technique for assessing the composition of comet dust in a large number of comets: 1) the peak thermal emission output from comet dust at $r_h \approx 0.5$–4.0 AU is

* Corresponding author.
Email addresses: msk@physics.ucf.edu (Michael S. Kelley), Diane.H.Wooden@nasa.gov (Diane H. Wooden).

at $\lambda \approx 7 - 20$ μm; 2) the mid-IR covers prominent emission features from silicate minerals, a major constituent of comet dust; and 3) only low to moderate spectral resolution ($\lambda/\Delta\lambda \gtrsim 100$) is required to critically assess the composition of comet dust. By studying the physical properties of dust ejected by comet nuclei, we gain insight into the formation mechanism of dust in the solar nebula, and the structure and dynamics of the proto-planetary disk (PPD).

Through comparisons between dust in the interstellar medium, interplanetary dust grains (Brownlee, 1985), comet dust, and asteroidal materials, we may attempt to ascertain the extent to which PPD processes altered pre-solar dust and mixed it throughout the comet forming zone (Wooden, 2008). Being a mixture of pre-solar and solar nebula processed material, measuring the composition of comet dust helps us understand both the origin of the constituents of the primitive solar system, and their subsequent evolution into planetesimals (Ehrenfreund et al., 2004; Wooden, 2008). In a similar vein, we can use JFCs to learn about the compositions of Scattered Disk objects since these bodies are dynamically linked (Duncan et al., 2004) and therefore their dust properties may be related. In contrast, Kuiper Belt objects from the classical disk likely formed in situ, and represent a population of icy bodies separate from the Scattered Disk objects and comet nuclei. Indeed, Kuiper Belt objects have redder surface colors, on average, than comet nuclei (Jewitt, 2002), indicating that they have a different origin or evolutionary history.

Since mid-infrared spectroscopy is effective at measuring comet dust properties, it offers important insight into the structure of the PPD. We can use mid-IR observations of comet dust to explore the heterogeneity of the PPD on sub-kilometer and super-kilometer (i.e., possibly tens of AU) scales by measuring the heterogeneity of comet nuclei. Dust may be ejected into the comet coma from a localized region on the nucleus at different epochs either by natural or unnatural processes, e.g., seasonal variations in insolation, outbursts, or collisions (*Deep Impact*-like events or natural). If the dust composition of the ambient coma differs from the localized regions, then we may conclude that the comet nucleus is heterogeneous. Nucleus heterogeneity could arise from the aggregation of varied planetesimals (see, e.g., Belton et al., 2007) and evidence for heterogeneity implies the proto-planetary disk in the comet forming regions was heterogeneous on kilometer to sub-kilometer sized scales (the typical radius of a comet nucleus is of order 1 km; Lamy et al., 2004). Alternatively, the dust properties of individual nuclei could be relatively homogeneous, yet the dust compositions vary from comet-to-comet. This second scenario favors PPD heterogeneities on the super-kilometer scale. A taxonomy of comets classified according to their dust properties has the promise to provide evidence supporting local (spatial or temporal) variations in dust composition in the comet forming region of the PPD. Evidence for chemical heterogeneity on both sub- and super-kilometer scales has been discovered through observations of comet gas species (Bockelée-Morvan et al., 2004), e.g., the C_2 comet classes (A'Hearn et al., 1995), the organic chemistry classes (Mumma et al., 2003; Bockelée-Morvan et al., 2004; Crovisier, 2007), the apparent CO variability of comet 21P/Giacobini-Zinner (Mumma et al., 2000; Weaver et al., 1999), and the CO_2 and H_2O composition of comet 9P/Tempel (Feaga et al., 2007).

In this paper, we review the composition of Jupiter-family comets as inferred from infrared spectroscopy: in §2 we review mid-IR spectroscopic observations of JFCs; in §3 we summarize and discuss observations of silicate mineralogy in JFCs, we demonstrate (§3.3) that the silicate feature strength is increased by subtracting emission from the nucleus, but not increased enough to match the strong silicate features of some OC comets, and from this perspective we discuss opportunities for important observations in the future; in §4 we review the mid-IR observations and models of comet 9P/Tempel in the context of the *Deep Impact* mission; in §5 we discuss the potential significance to our understanding of PPD processes of the detection of hydrated and Fe-rich minerals identified in comet 9P/Tempel; and, in §6 we summarize the review.

2. Mid-infrared Spectroscopic Observations

Mid-infrared spectra, with $\lambda/\Delta\lambda \gtrapprox 50$, exist for 13 Jupiter-family comets and these observations are summarized in Table 1. We also list whether or not a silicate emission feature was detected above the continuum for each spectrum, and the strength of that feature, if available. It is important to note that the 10 μm continuum in a mid-IR spectrum of a comet is composed of thermal emission from dust species that exhibit little variation in emissivity with wavelength for $\lambda = 7 - 14$ μm. The common "continuum" contributers are amorphous carbon, FeS, and grains large enough to be optically thick to 10 μm emission (Hanner et al., 1994; Wooden, 2002). Thermal emission from the nucleus can also be an important source of continuum flux, and should be removed before measuring the silicate emission (see §3.3). A silicate feature has been detected in 8 of the 13 comets in Table 1, and the typical silicate emission band strength is 1.20–1.25. The silicate emission band strength is computed from the ratio of the mean in-band flux between 10.0 and 11.0 μm to a scaled Planck function that is fit to small sections of the smooth continuum at $\lambda \leq 8.2 - 8.4$ μm and $\lambda \geq 12.4 - 12.5$ μm and evaluated at 10.5 μm (Hanner et al., 1996; Sitko et al., 2004; Sugita et al., 2005). Observed silicate band emission strengths in Oort Cloud comets range from 1.0 to 4.0 (Hanner et al., 1994; Williams et al., 1997; Harker et al., 1999; Sitko et al., 2004). Such strong silicate band emission has not been observed in a JFC, except in the post-*Deep Impact* coma of 9P/Tempel (Lisse et al. 2006; Harker et al. 2007; §4).

The *Spitzer Space Telescope* (Werner et al., 2004; Gehrz et al., 2007) has significantly increased the number of spectroscopic observations of JFCs in the mid-IR. Three comets with high-quality spectra are listed in Table 1, and 9 more

are briefly summarized by Kelley (2006). This boon to JFC spectroscopy is largely attributable to the high sensitivities of the Infrared Spectrograph (IRS) instrument (Houck et al., 2004) and the high observing efficiency of the *Spitzer* spacecraft. As future infrared space telescopes will have larger primary mirror diameters, such as the JAXA *Space Infrared Telescope for Cosmology and Astrophysics* (*SPICA*), and the NASA *James Webb Space Telescope*, bright comets may become unaccessible to space-borne instrumentation. Instead, ground-based and airborne telescopes will be used to observe the brightest comets.

Ground-based observations account for 1/2 of the spectra in Table 1; about 2/3 of those spectra were taken at the NASA's 3 m Infrared Telescope Facility (IRTF). Eight meter telescopes hold great promise for the spectroscopic investigation of JFCs. The Gemini and Subaru telescopes have already provided three definitive detections of crystalline silicates in JFCs; the measured crystalline-to-amorphous sub-μm mass ratios are: $\sim$0.9 for 78P/Gehrels (Watanabe et al. 2005; also discussed in Ootsubo et al. 2007a), 0.3–0.8 for 9P/Tempel (Harker et al., 2005, 2007; Sugita et al., 2005; Lisse et al., 2006), and qualitatively described as less than in Hale-Bopp for 73P/Schwassmann-Wachmann (Harker et al., 2006b; Sitko et al., 2006d). Also, Gemini-N and Subaru observations of the *Deep Impact* event provided, in part, the evidence for the heterogeneous structure and composition of the nucleus of 9P/Tempel (Harker et al., 2007; Kadono et al., 2007). With the continued use of mid-IR instruments on large telescopes, and in conjunction with the archive of space-based observations, we can increase the number of high-quality spectra of JFCs to statistically significant numbers, which will give us the opportunity to establish the extent of crystalline silicate enrichment in JFCs and the degree of JFC nucleus heterogeneity.

Future airborne instrumentation on the Stratospheric Observatory for Infrared Astronomy (SOFIA) will cover mid-IR wavelengths in spectroscopy mode (Becklin et al., 2007). With the telescope executing science operations at altitudes $\gtrapprox$ 12.5 km, SOFIA will be an important resource for comet astronomy at 15–40 μm, where atmospheric absorption greatly interferes with observations at ground-based observatories. At these wavelengths, the spectral resonances of crystalline silicates are more separated in wavelength, and therefore more distinct, than the resonances near 10 μm. With 15–40 μm spectra, we can accurately measure the mineralogical makeup of silicate crystals in a comet's coma by measuring the central positions and strengths of the crystalline emission resonances. In particular, the Fe to Mg ratio of silicate crystals is better constrained when the longer wavelength peaks are measured. SOFIA will add vital observations to the few crystalline measurements made at these wavelengths.

3. Silicates in Jupiter-Family Comets

3.1. *Properties of silicate grains and their thermal emission*

Silicate minerals in comets have prominent emission features in the mid-IR. Molecular bonds between Si and O atoms have stretching and bending modes that produce emission at 8–12 μm and at 15–40 μm, respectively. The central wavelengths, relative strengths, and shapes of these features are diagnostic of the mineral composition. Wooden (2002) reviews the silicate minerals observed in ground-based mid-IR spectra of comets: $[Mg_y,Fe_{1-y}]_2SiO_4$ (olivine) and $[Mg_x,Fe_{1-x}]SiO_3$ (pyroxene), where x and y range from 0 (Fe-pure: fayalite and ferrosilite) to 1 (Mg-pure: forsterite and enstatite). Cometary silicates are found in both amorphous (non-stoichiometric) and crystalline structures. An example of the narrow thermal emission resonances attributed to silicate crystals, and the broad emission attributed to amorphous grains is presented in Fig. 1.

Comet comae are optically thin to mid-IR radiation. In order to detect the thermal emission from silicate grains in a dust coma, the grains must be in sufficient quantities to be detected above the observational uncertainty of the smooth thermal continuum (Hanner et al., 1994). Aside from the amount, each grain's size, composition, and structure play important roles in the strength of the silicate emission, primarily by determining the grain equilibrium temperature. We discuss each of these properties (size, composition, and structure) in turn.

First, dust grain size affects the grain temperature. Sub-μm sized grains have higher temperatures than (solid) grains larger than 1 μm of the same composition. The temperature difference arises from the dependence of grain emission efficiency on grain size. All silicate dust grains greater than 0.1 μm in size are efficient absorbers of sunlight at visible wavelengths (the peak of the solar output), but the sub-μm sized grains are inefficient emitters in the mid-IR. Since grain radiative cooling at $r_h \approx 0.5-4$ AU is dominated by mid-IR radiation, the temperatures of sub-μm sized grains are warmer, which subsequently increases their total thermal emission flux.

In contrast with grain size, which primarily affects the emission efficiencies of comet grains, composition affects grain absorption efficiencies. Increasing the amount of Fe in a silicate grain (decreasing Mg) increases the grain's absorption efficiencies at visible and near-IR wavelengths, which in turn increases the grain's equilibrium temperature (Dorschner et al., 1995). The higher temperatures cause Fe-rich grains to be easier to detect by spectroscopic means, yet Harker (1999) found the grain temperatures of amorphous silicates in comet Hale-Bopp were best-modeled with roughly equal amounts of Mg and Fe ($x = y = 0.5$). Furthermore, Harker (1999) found the silicate crystals to be distinctly Mg-rich ($x = y = 0.9 - 1.0$). These grain parameters have been commonly used by other investigations

(Moreno et al., 2003; Honda et al., 2004; Min et al., 2005; Harker et al., 2007). However, Lisse et al. (2006) found significant amounts of Fe-rich pyroxene in the *Deep Impact* ejecta from comet 9P/Tempel (see §4 and Fig. 4). In Fig. 2, we summarize the variation of the peak wavelength position with Mg content for strong crystalline olivine and orthopyroxene peaks observed near 10 μm from the analyses of Koike et al. (2003) and Chihara et al. (2001).

Finally, grain structure (i.e., porosity and shape) influences the thermal emission from dust. For two otherwise similar grains, increased porosity will produce a warmer equilibrium temperature and, in larger grains, a stronger 10 μm silicate emission feature (Hage and Greenberg, 1990; Xing and Hanner, 1997; Min et al., 2006; Kolokolova et al., 2007; Voshchinnikov and Henning, 2008). The effect is due to insulating vacuum inside porous grains, causing sub-domains to be increasingly thermally isolated from each other. If the porosity of an aggregate grain is more than 63% then the temperature begins to approach that of the monomer ($\sim$0.1 μm sub-grains): at 80% porosity the temperature of the aggregate is only 4–6% lower than a monomer (Xing and Hanner, 1997). Also, the shape of a porous aggregate determines whether larger porous grains lose or retain their silicate resonant features (Kolokolova et al., 2007). The net result of increased porosity is a thermal emission spectrum with a hotter temperature and a stronger silicate feature compared to a similar sized compact grain. Thermal emission models for porous aggregates that include crystals (computed with the Discrete Dipole Approximation; Moreno et al., 2003) yield similar crystalline fractions as the less time-intensive approach of modeling a grain distribution composed of discrete crystals and mono-mineralogic porous grains (Harker et al., 2002, 2004a).

The above three grain parameters (size, composition, and structure) all affect the observed *strength* of a coma's silicate emission feature, but each parameter also affects the *shape* of the feature. When we consider the silicate emission feature's shape, and the shape of the entire spectrum, we find that there are no one-to-one degeneracies among the dust grain parameters, although there are consistent trends. For example, the silicate feature strength can be raised by increasing the porosity of grains above $\sim$ 80% vacuum, which yields silicate features and temperatures similar to their monomers (Xing and Hanner, 1997). Increasing the porosity of dust grains in a coma also shifts the spectral slope of the Rayleigh-Jeans side of the observed spectrum towards the blue (i.e., there are fewer, cool grains contributing to the flux at long wavelengths). A small portion of this change in spectral slope can be accounted for by flattening the size distribution to increase the relative number of larger, cooler grains. The entire effect, however, cannot be accounted for in this manner—this is evident when we consider that the largest, highly porous grains have higher equilibrium temperatures than the largest grains with more compact shapes. Oort cloud comet Hale-Bopp is an example of a comet that displays an extremely strong silicate feature, and that fitting its spectrum requires a size distribution that possesses both highly porous grains and very small grains (peak grain radius of 0.15–0.2 μm; Harker et al., 2002; Moreno et al., 2003; Min et al., 2005). Wooden (2002) discusses how comet Hale-Bopp's grain porosity and grain size distribution slope are each constrained by spectra. In another example, Oort Cloud comet C/2001 Q4 (NEAT) has a silicate feature identical in shape to, but weaker in strength than, that of Hale-Bopp (Wooden et al., 2004). In fact, Q4's silicate feature strength varies on short times scales and is best explained by a variable silicate-to-amorphous carbon mass ratio (Wooden et al., 2004; Harker et al., 2004b). Specifically, decreasing the silicate feature strength by a factor of 1.5 by removing the grains smaller than 0.6 μm broadens the shape of the silicate feature more than what is observed for Q4. Therefore grain size effects cannot explain the observed variations in the spectra of comet Q4.

With the above arguments in mind, we can consider the positive detection of silicate features in many JFCs (Table 1) and draw some conclusions. The weak silicate band emission in JFCs, as compared to some OC comets, could be due to: 1) silicates may be less abundant with respect to other dust components (e.g., amorphous carbon, FeS) in JFCs than in OC comets; 2) silicate grains may be larger in JFCs than in OC comets; 3) JFC dust may be less porous than OC comet dust; or 4) a combination of 1, 2, and/or 3. Out of the few JFCs that have been studied in-detail, there is no clear agreement in the silicate dust content of their comae. Kelley et al. (2006) found Jupiter-family comet 2P/Encke had a peak grain size distribution of 0.4–0.5 μm and a sub-μm silicate dust mass fraction of $< 31\%$ (3σ upper-limit). Hanner et al. (1996) reasonably reproduced the silicate feature of 19P/Borrelly to within 10% using a 50-50 mixture of silicates and carbon. Models of pre-*Deep Impact* spectra of 9P/Tempel favored a silicate dust distribution with a peak grain size of 0.7–0.8 μm for solid to somewhat porous grains (Harker et al., 2007). It may be that these three comets are truly different in their compositions and grain size distributions, however the models could be refined with new or improved constraints. For example, the comet Encke model fits could benefit from higher sensitivity spectra at $\lambda < 14$ μm that better constrain the grain temperatures and silicate compositions, and all three comet models could be improved with constraints derived from scattered light observations (§3.2). Thermal emission modeling has the potential to constrain grain parameters, but only within the limitations of a given data set.

A few OC comet thermal emission spectra have also been modeled. Models of comets C/2001 Q4 (NEAT), C/2002 V2 (NEAT), and Hale-Bopp reveal comae with smaller peak grain sizes (0.1–0.5 μm) that are dominated by crystalline silicate grains (see Ootsubo et al., 2007a, and references therein). Hanner et al. (1994) find that weak silicate emission in several OC comets is correlated with a weak dust scattering continuum and weak 3 μm thermal emission, altogether suggesting a lack of small grains. From the thermal

emission studies it is not clear which of the possible causes (1, 2, or 3) manifest the differences between comet mid-IR spectra, but, from the limited results above, OC comets seem to have an abundance of the smallest grain sizes, when compared with JFCs. In the next section we present recent developments in models of light scattered by comet dust that suggest grain porosity is the dominant property.

3.2. *Grain Porosity, Thermal Emission, and Light Scattered by Comet Dust*

Models and observations of light scattered by comet dust, in tandem with mid-IR observations, are providing intriguing evidence that supports grain structure as the dominant cause for the difference between JFCs and OC comets. In light scattering models, grain structure refers to one of three types: solid grains; compact porous aggregates, described by ballistic particle-cluster aggregation (BPCA); or, fluffy (highly porous) aggregates, described by ballistic cluster-cluster aggregation (BCCA) (Mukai et al., 1992). Grain structure affects the strength of the silicate feature, polarization, and surface brightness radial profiles (the latter due to the changing efficiencies of gas drag and the solar radiation force; Meakin and Donn, 1988; Mukai et al., 1992; Nakamura et al., 1994).

Kolokolova et al. (2007) delineate two types of dust comae: 1) comae dominated by compact grains that are either solid, or compact porous; or 2) comae dominated by fluffy aggregates. In scattered light models (Kimura et al., 2003; Kimura and Mann, 2004; Kimura et al., 2006), both grain types reasonably reproduce the observed optical properties of comet dust (for a review, see Kolokolova et al., 2004), but one observable breaks the degeneracy: the relationship between the 10 μm silicate emission and the structure of the aggregates.

Kolokolova et al. (2007) show that the surface brightness distributions of the dust and gas in comet comae vary from comet-to-comet. They suggest that gas-rich comets have dust comae that are more spatially compact than their gas comae (e.g., comet Encke, Jockers et al., 2005), and dusty comets have dust and gas comae with similar surface brightness distributions. Gas-rich comets have lower optical polarization maxima than dusty comets, and the low optical polarization is correlated with weak or absent 10 μm silicate features (Levasseur-Regourd et al., 1996). Exploiting the correlation between low optical polarization and dust surface brightness distribution, and using recent observations that have shown the low optical polarization is due to gas contamination in broadband filters (Kiselev et al., 2004; Jewitt, 2004; Jockers et al., 2005), Kolokolova et al. (2007) develop a physical explanation to describe the correlation between dust-to-gas ratios and the 10 μm silicate emission feature. Their argument is as follows: 1) fluffy, porous aggregates have stronger or equivalent 10 μm silicate emission features compared to compact, or solid, aggregates (summarized above); 2) fluffy aggregates should be more easily accelerated to the gas outflow velocity than compact grains, primarily due to their larger surface areas per mass (Meakin and Donn, 1988; Nakamura et al., 1994); 3) in constrast, compact grains are not accelerated to the gas expansion velocity, and dust comae consisting of compact grains will be more concentrated around the comet nucleus than the gas. Altogether, the scattered light and the thermal emission properties of comet dust suggest that grain porosity could be the predominant characteristic that determines the strength of the comet's silicate features.

3.3. *The influence of the nucleus on observed silicate band strength*

When assessing the dust content of comet comae, it is important to remove the contribution of the nucleus from the total thermal emission flux. The nucleus can be a dominant contributor to the mid-IR flux of JFCs, which are typically less active than their Oort Cloud counterparts (A'Hearn et al., 1995). A large nucleus flux skews the silicate band strength towards lower values. To illustrate this fact, we estimate the fraction of the mid-IR flux attributable to the nucleus in a typical JFC observed at $r_h = 1.8$ AU. We will base our model comet on surveys of JFC dust production rates (A'Hearn et al., 1995) and nucleus sizes (Lamy et al., 2004). We will also "observe" our model comet at $r_h = 1.0$ AU by appropriately increasing the dust production rate and phase angle to show how the nucleus fraction varies with heliocentric distance. We then examine Table 1 to determine if the weak silicate features are actually a product of large nuclei with low dust production rates.

Since visible light observations of comets are more readily available than mid-IR observations, it is advantageous to use the visible observations to estimate the coma brightness of a typical JFC. The visible light proxy for dust production is the quantity $Af\rho$, where A is the Bond albedo of the dust, f is the dust areal filling factor in the field-of-view, and ρ is the projected radius of the field-of-view, typically expressed in units of cm (A'Hearn et al., 1984). The filling factor may be expressed as $f = N\sigma\pi^{-1}\rho^{-2}$, where $N\sigma$ is the total cross-section of the grains in cm^2. Technically, f depends on the extinction cross-sections of the grains and not on the geometric cross-sections (A'Hearn et al., 1984). For comae with constant isotropic outflows, $Af\rho$ is independent of aperture size.

The thermal emission, F_λ in units of W cm^{-2} μm^{-1}, from a collection of isotropically emitting isothermal grains is

$$F_\lambda = (1 - \bar{A})\ \pi B_\lambda(T)\ f\frac{\rho^2}{\Delta^2}, \quad (1)$$

where $\bar{A}$ is the mean bolometric albedo of the dust (≈ 0.32; Gehrz and Ney, 1992), $B_\lambda(T)$ is the Planck function in units of W cm^{-2} μm^{-1} sr^{-1} evaluated for the grain temperature T and at a wavelength of λ, and Δ is the comet-observer distance in cm. It is useful to express Eq. 1 in terms of $Af\rho$

and θ, where $\theta = 206265\ \rho\ \Delta^{-1}$ is the angular size of the aperture in units of arcseconds,

$$F_\lambda = \frac{(1-\bar{A})}{A(\alpha)}\ \pi B_\lambda(T)\ \frac{\theta}{206265}\ \frac{A(\alpha) f\rho}{\Delta}. \quad (2)$$

Here, we explicitly write the phase angle dependence of the albedo as $A(\alpha)$; the thermal emission term, $1-\bar{A}$, is independent of phase angle. Visual albedo measurements of Jupiter-family comets are rare. We found that only one comet, 21P/Giacobini-Zinner, has been studied, and it has a low albedo: $A(64^\circ) = 0.07 - 0.15$ (Telesco et al., 1986), $A(22^\circ) = 0.11$ (Pittichova et al., 2008). In the near-IR, JFCs have albedos equivalent to or lower than Oort Cloud comets (Campins et al., 1982; Hanner and Newburn, 1989). Since comets are typically observed at low-to-moderate phase angles, we have chosen $A(\alpha < 60^\circ)$ to be 0.15, which is slightly under the apparent mean $A(\alpha)$ of several Oort Cloud comets (see Fig. 1 of Kolokolova et al., 2007). The mid-IR coma flux is fairly sensitive to $A(\alpha)$, therefore measured values should be used when possible. Assuming a value of 0.15 introduces a factor of 2 uncertainty in the mid-IR flux when we consider the observed range is $\approx 0.1 - 0.25$ (excluding comet Hale-Bopp; Kolokolova et al., 2004). We take the ensemble average dust temperature to be 10% warmer than the blackbody temperature, T_{BB}, at the observed r_h,

$$T \approx 1.10\ T_{BB} = \frac{306\mathrm{K}}{\sqrt{r_h}}, \quad (3)$$

which is within the typical range (0–30%) observed in many comets (Gehrz and Ney, 1992; Hanner et al., 1996).

The near-Earth asteroid thermal model (Harris, 1998) has proven to be sufficient for modeling the thermal emission from comet nuclei, although with some modifications. Groussin et al. (2004) suggests an IR-beaming parameter of 0.85 for comets, based on the surface models of Lagerros (1998). In the formalism of the near-Earth asteroid thermal model, the beaming parameter contributes to the observed effective temperature of the nucleus. The value of 0.756 has been favored for large, main-belt asteroids (Lebofsky et al., 1986), but equivalent or larger values, up to ≈ 1.0, have been experimentally determined with infrared observations of comet nuclei (Fernández et al., 2000; Kelley et al., 2006; Fernández et al., 2006; Groussin et al., 2007). We adopt 0.85 throughout our paper. We also use a geometric albedo of 0.04, a typical value for comet nuclei (Lamy et al., 2004).

A'Hearn et al. (1995) surveyed the optical properties of 85 comets, of which 34 belong to the Jupiter-family class. Their median observed $Af\rho$ value for JFCs is 110 cm at a median r_h of 1.8 AU. We derive a median nucleus radius of 1.8 km for the 34 JFCs using the radii listed by Lamy et al. (2004) and updated values for 81P/Wild and 9P/Tempel from Brownlee et al. (2004) and A'Hearn et al. (2005). Table 2 lists the nucleus-to-coma flux ratios at 10 μm for various observing parameters of our median JFC ($Af\rho = 110$ cm, $r_h = 1.8$ AU, $R_n = 1.8$ km). Of course, our fictional "median JFC" parameters are not representative of any particular JFC, and that spectra of each comet should be considered on a individual basis. Table 2 also lists estimates for the median JFC observed at $r_h = 1.0$ AU by scaling the $Af\rho$ value up by a factor of $1.8^{2.3}$, as suggested by A'Hearn et al. (1995).

A bright nucleus may affect derived coma parameters, the most immediate of which is the silicate band strength. It is clear from Table 2 that the nucleus flux can comprise a significant amount of the total flux measured in mid-IR spectra, as high as 80–90%, especially when observing comets with low dust production rates ($Af\rho \approxeq 100-200$ cm) using the narrow-slits (0.4–1.0″ wide) on ground-based instrumentation. In this case, if the silicate band strength appears to be between 1.10 and 1.30, then the nucleus subtracted (corrected) silicate band strength would lie between 1.50 and 3.0! With a larger slit, the nucleus could be 10–30% of the flux. The corrected silicate band strength would then increase to 1.11–1.43. The latter small changes in the silicate band emission of a JFC may not be significant when comparing a JFC to comet Hale-Bopp, which had a silicate emission feature that ranged from 3.0 to 4.0, but are important when assessing the properties of JFCs as a whole.

Removing the nucleus is relevant to grain thermal emission modeling, even in comets with no discernible silicate emission feature. Comet nuclei have temperature distributions unlike collections of isothermal grains (the dust coma). Comet nuclei have low thermal inertia (e.g., Groussin et al., 2007), therefore, the sub-solar point on a slowly rotating nucleus will be hottest, and the temperature decreases as the sun-zenith angle ($\theta_\odot$) increases (in the near-Earth asteroid model, $T \propto \cos^{1/4}\theta_\odot$). In contrast, the thermal propagation timescales in small grains are fast and they quickly equilibrate to a single temperature—a temperature that is cooler than the effective temperatures of comet nuclei. Thus, the shortest wavelengths of a thermal emission spectrum will include the highest fraction of flux from the nucleus (e.g., see the reduction of the 2P/Encke spectra in Kelley et al., 2006). If the nucleus emission is not removed, a coma modeler would find an increased number of the smallest grains (the grain sizes that are constrained by the shortest wavelengths) over a best-fit model that excludes the nucleus flux.

We now refer to Table 1 and discuss our estimates of how the thermal emission from each comet's nucleus affects the observed silicate band strength. Hanner et al. (1996) considers the size of the comet nucleus when computing the silicate band strength of comet 4P/Faye, so no correction is necessary. Based on images of the nucleus of comet 19P/Borrelly (Buratti et al., 2004), the 8.0×3.2 km prolate nucleus contributes 14–36% of the flux in the spectrum of Hanner et al. (1996). The silicate emission feature strength is reported by Hanner et al. (1996) to be ≈ 1.25. Their plot of the data, however, suggests that ≈ 1.11 is a more appropriate value. Removing the nucleus flux increases the strength to 1.13–1.19. Stansberry et al. (2004) estimate the silicate band strength of comet

29P/Schwassmann-Wachmann to be approximately 1.10. We use their model nucleus parameters and derive a corrected band strength of 1.19. Sitko et al. (2004) observed 69P/Taylor and find the silicate band strength to be 1.23. The radius of 69P is estimated to be 2.1 ± 0.6 km by Tancredi et al. (2006), which corresponds to 4–19% of the thermal emission in the Sitko et al. (2004) mid-IR spectrum. The result is a minor increase in the the silicate band strength to 1.24–1.28. The silicate band strength of comet 103P/Hartley (1.20) measured by Crovisier et al. (2000) requires no correction due to the large aperture of the ISOPHOT instrument ($24'' \times 24''$), and the small nucleus size, $R_n = 0.71 \pm 0.13$ km (Groussin et al., 2004). We derive a nucleus contribution of $\leq 1\%$ for comet 103P. Finally, the observation of 103P/Hartley by Lynch et al. (1998) requires a minor correction, resulting in an increase of the measured silicate band strength from 1.15 to 1.22, which matches the ISOPHOT derived silicate band strength.

4. Comet 9P/Tempel and *Deep Impact*

Comet 9P was the primary target of the *Deep Impact* mission—a mission designed to impact a comet nucleus to determine its underlying strength, structure, and composition. In all ways, comet 9P/Tempel is considered to be a typical JFC (A'Hearn and Combi, 2007). The *Deep Impact* spacecraft delivered a 370 kg impactor into the nucleus of 9P/Tempel at a relative velocity of 10.3 km s^{-1}. The fly-by spacecraft observed the event from a distance of 500 km (A'Hearn et al., 2005). The impact excavated $\sim 10^5 - 10^6$ kg of ice and dust from the surface and interior of the comet (Sugita et al., 2005; Harker et al., 2005; Küppers et al., 2005; Keller et al., 2007).

Some of the most detailed mid-IR spectra of any JFC were obtained of comet 9P/Tempel in support of the *Deep Impact* mission. Three investigations have been presented: 1) *Spitzer* observations of the pre- and post-impact coma (approximately 30 and 60 min after impact) at 5–40 μm (Lisse et al., 2006); 2) Gemini-N observations of the pre- and post-impact coma (approximately 7 min cadence for 3 hr, and additional spectra 24 hr after impact), primarily at 8–13 μm (Harker et al., 2007); and 3) a Subaru observation of the post-impact coma (3.5 hr after impact) at 8–13 μm (Ootsubo et al., 2007b).

4.1. *The Pre-Deep Impact Dust Coma*

The *Deep Impact* spacecraft studied the ambient coma and nucleus of comet 9P and provided excellent context for observations from other spacecraft and ground-based observatories. Farnham et al. (2007) analyzed images of 9P/Tempel taken by the *Deep Impact* spacecraft and found that the pre-impact dust coma has three prominent jets, the strongest of which originates near comet 9P's south pole. Feaga et al. (2007) observed CO_2 and H_2O gas in the coma and find that CO_2 is preferentially ejected from the southern pole (correlated with the dust) and that H_2O is preferentially ejected in the sunward direction (on the northern hemisphere at the time of observation). The CO_2 and H_2O asymmetries gives strong evidence for either differentiation of ices in the nucleus, or primordial heterogeneity. Comet jets will typically be unresolved in mid-IR observations, but it would be interesting to investigate whether dust from 9P's discrete sources propagate into separate coherent coma or tail structures (Farnham et al., 2007), and if the dust properties of these structures could be assessed using the high signal-to-noise spectral map of comet 9P taken with the *Spitzer*/IRS instrument. For the purposes of this review, we will assume analyses of mid-IR observations of the pre-*Deep Impact* coma probe a global average of the dust properties of this comet.

Lisse et al. (2006) present a pre-impact *Spitzer* spectrum of 9P/Tempel, but a detailed analysis of this spectrum is not given. In Fig. 3 we present the pre-impact spectrum taken by *Spitzer* on 03 July 2005. A model nucleus has been removed, and a silicate feature (strength of $\approx 20\%$) is clearly observed at 8–12 μm. We estimate the silicate band strength to be in the range 1.19–1.25.

Harker et al. (2007) describe their pre-impact Gemini spectra as "essentially smooth and nearly featureless" with a silicate band strength close to 1.0 (no silicate emission), although an uncertainty is not presented (the nucleus also amounts to 80% of their pre-impact flux). We estimate the silicate band strength to be 1.2 ± 0.2 (after nucleus subtraction). A spectrum taken in May 2005, about 1.5 months prior to the *Deep Impact* encounter, did show clear silicate emission (we estimate the strength to be 1.50 ± 0.18). In May 2005 when dust from the southern jet dominates the coma (Farnham et al., 2007), the dust mineralogy is dominated by solid (zero porosity) amorphous pyroxene silicates with a peak grain size of 0.7 μm, whereas in July 2005 pre-impact the ambient coma is comprised of moderately porous (46% vacuum for a 10 μm grain) amorphous carbon and amorphous olivine silicates with a slightly larger peak grain size of 0.8 μm. Note that for a 10 μm radius grain, the silicate feature strength increases from negligible to ≈ 1.2 as the porosity changes from solid (0% vacuum) to moderately porous ($\approx$50% vacuum) (Harker et al., 2002, 2007). In summary, JFC comae with low dust production rates or measured through small slits may at first appear to have "featureless" IR spectra (especially at low signal-to-noise ratios), but modeling after nucleus removal can reveal micron-sized solid or 10 μm porous silicate grains, as is the case for pre-impact comet 9P (Figs. 2 and 5 of Harker et al., 2007).

4.2. *The Post-Deep Impact Dust Coma*

Post-impact mid-IR spectra were dramatically different from the pre-impact spectra (Fig. 3). Mid-IR spectra of the ejecta show the strong resonances of sub-μm sized crystalline silicates of both olivine and pyroxene grains (Lisse et

al., 2006; Harker et al., 2007; Ootsubo et al., 2007b). This discovery is perhaps the most immediate result of the mid-IR investigations. A *Spitzer*/IRS observation of the 10 μm silicate feature (0.64 hr after impact) is presented in Fig. 2. We find the post-impact silicate band emission strength to be near 2.0 (both the Gemini and *Spitzer* observations; see column 6 in Table 1), the strongest feature ever observed in a spectrum of a JFC. The derived crystalline-to-amorphous silicate sub-μm mass ratios range from approximately 0.2 to 4 (Harker et al., 2005, 2007; Lisse et al., 2006; Ootsubo et al., 2007b). The values depend on slit width, orientation, and time of observation, which could easily explain the wide range of values. The pre-impact crystalline-to-amorphous silicate ratio has not been significantly constrained ($\lesssim 1.6$, 1σ upper-limit Harker et al., 2007).

Only in two or three other JFCs, 78P/Gehrels (Watanabe et al., 2005), 73P/Schwassmann-Wachmann (Harker et al., 2006b), and, possibly, 103P/Hartley (Crovisier et al., 2000), have detections of crystalline silicates been reported. We may also include the Centaur-like JFC 29P/Schwassmann-Wachmann (Stansberry et al., 2004). For comparison with 9P, Watanabe et al. (2005) found a crystalline-to-amorphous silicate ratio of $\approx$ 0.9 for 78P/Gehrels. The crystalline-to-amorphous silicate ratios of 78P and the *Deep Impact* ejecta are significantly greater than that found in the interstellar medium, ≤ 0.022, (Kemper et al., 2004, 2005), and similar to or smaller than the crystalline-to-amorphous ratios measured in the comae of some Oort Cloud comets (2–3 for comets Hale-Bopp, C/2001 Q4 (NEAT), and C/2002 V1 (NEAT); Harker et al., 2002, 2004a; Wooden et al., 2004; Ootsubo et al., 2007a).

Aside from the crystals, Harker et al. (2007) find that the *Deep Impact* ejecta was rich in amorphous pyroxene, in contrast with the amorphous olivine and amorphous carbon dominated pre-impact coma in July 2005, but similar to the higher dust production rate coma in May 2005. In the impact-induced coma, crystalline olivine is correlated with the amorphous pyroxene dust, suggesting these minerals originated from the same reservoir (the *Deep Impact* crater). Harker et al. (2007) also found a population of amorphous carbon grains traveling at a projected speed of 700 m s $^{-1}$, equivalent to the highest speed ejecta seen by other observers (see, e.g., Keller et al., 2007). Schultz et al. (2007) interpret high speed ejecta as originating from the upper 5 m of the nucleus, whereas slower ejecta is from deeper layers. Harker et al. (2007) and Kadono et al. (2007) conclude that the surface of the nucleus is rich in sub-μm amorphous carbon grains.

With the broad wavelength coverage of *Spitzer* (5–40 μm), Lisse et al. (2006) were able to identify a number of minerals that have not been previously reported in cometary spectra, namely Fe-rich silicates, metal sulfides, phyllosilicates, and carbonates. To emphasize the benefit of the long wavelength coverage, we assembled a bar chart consisting of 9P/Tempel's dust components (Fig. 4). The figure highlights those minerals that in principle are difficult to constrain without the 5–40 μm *Spitzer* spectra—these components add up to one-third of the total dust surface area. Lisse et al. (2006) find that 8% of all the silicates by emitting surface area are in the form of the Fe-rich hydrated mineral nontronite, and 5% of the total surface area is in the Mg-rich carbonate magnesite, or the Fe-rich carbonate siderite. In §5.1, we discuss implications of the presence of hydrated minerals on our knowledge of comet nuclei.

Harker et al. (2007) and Ootsubo et al. (2007b) assumed a Mg-rich composition for their crystalline silicate grains, which allowed adequate fits to most of their spectra ($\chi^2 \lessapprox 1.0$). Lisse et al. (2006) simultaneously fit both Mg-rich and Fe-rich silicate minerals to their spectra and find significant amounts of Fe-rich silicate crystals. By number, the olivine Fe-/Mg-rich ratio is 0.3, and the pyroxene Fe-/Mg-rich ratio is 3.1. The difference between the Fe-/Mg-rich ratio in these two major silicate groups is intriguing. Both comets 9P and Hale-Bopp have high crystalline silicate fractions, but their specific minerals are different. Only the Mg-rich species were present in comet Hale-Bopp (Wooden et al., 1999; Bradley et al., 1999; Harker et al., 2002). Furthermore, an 11.25 μm peak in the spectra of other OC comets indicates Mg-rich grains (Hanner et al., 1994). As discussed below (§5.2), if aqueous water was not present in the comet nucleus (§5.1), then the Fe content of silicate minerals may be a gauge of the amount of water vapor present in the solar nebula during silicate crystal formation. Future observations and analysis of crystals in Jupiter-family and other comets from *Spitzer* and SOFIA are vital to our understanding of the origin and evolution of dust in our solar system.

5. The Implications of Hydrated Minerals and Fe-Rich Crystals on Dust Formation and Comet Evolution

5.1. *Hydrated Minerals*

The suggestion that Fe-rich crystalline silicates, phyllosilicates, and carbonates are components of comet dust has consequences on our understanding of dust formation and cometary evolution. Significant amounts of liquid water would be required if these minerals were to have formed in 9P/Tempel's nucleus (Lisse et al., 2006). This would upset the common understanding that the interiors of comets remained at low temperatures after formation (Meech and Svoreň, 2004). Carbonates are thought to form by aqueous alteration inside asteroids (Armstrong et al., 1982; Zolensky and Browning, 1997), because under steady-state conditions in the PPD mid-plane, the nebular concentration of CO_2 is too low (Lewis et al., 1979). The (anhydrous) mineral olivine could have been aqueously altered to become the phyllosilicate serpentine in water-rich shocks in the solar nebula phase Ciesla et al. (2003); Fegley and Prinn (1989). In contrast to the relatively simple incorporation of

the OH− radical into olivine to form serpentine, the formation of smectite requires mobilization of refractory element cations including Ca, Mg, and Si. The gas transport of refractory elements requires very high temperatures and this seems inconsistent with a shock-wave producing low temperature mineral phases such as phyllosilicates (A. Krot, private communication). Hence, phyllosilicates other than serpentine probably formed in the interiors of asteroids where pressures were higher than in the nebula (Alexander et al., 1989; Brearley, 2006; Scott and Krot, 2005).

To aqueously alter minerals in the comet nucleus, some mechanism must warm the comet interior enough to melt or sublime water ice. Deeper than a few km, heating by ^{26}Al is sufficient to crystallize amorphous water ice, but much of the excess heat is quickly dissipated due the the higher heat conductivity of crystalline ice (about 20 times the heat conductivity of amorphous ice). Only in comets with radii greater than 10 km can the temperature continue to rise to allow for liquid water to form (Prialnik and Podolak, 1995, 1999; Prialnik et al., 2008; Merk and Prialnik, 2006; McKinnon et al., 2008). The interior may be high enough to form phyllosilicates by aqueous alteration of silicate mineral grains in comet dust, but not hot enough to dry out the phyllosilicates to form FeO-rich crystalline silicates, as has been suggested to occur in asteroids (Krot et al., 1995, 2000). In addition to phyllosilicates, other minerals that characterize parent-body aqueous alteration include hydroxides, hydrated sulfides, sulfates, oxides, and carbonates (Zolensky and Browning, 1997). These secondary minerals are notably absent from comet 1P/Halley (Jessberger et al., 1988; Jessberger, 1999) and *Stardust* (Brownlee et al., 2006; Zolensky et al., 2006, 2007). The Lisse et al. (2006) analysis of comet 9P suggests low concentrations of carbonates and the phyllosilicate nontronite (a smectite), at the ≈5–10% level in comet 9P, but the identification of these minerals in spectra of other comets is still under study (Woodward et al., 2007; Bockelee-Morvan et al., 2007; Lisse et al., 2007). In an analysis of spectra of comet Hale-Bopp, (Wooden et al., 1999) set a tight constraint of $\leq 1\%$ on the phyllosilicate montmorilonite (a smectite). Note that radiogenic temperatures in comet nuclei are not sufficiently high, nor the conditions "dry" enough, to anneal and crystallize amorphous refractory silicate minerals in comet dust. As described before, crystalline grains appear to have formed prior to the accretion of comet nuclei.

5.2. *Fe-Rich Silicate Crystals*

Since the discovery of crystalline silicates in comets (Campins and Ryan, 1989), it has been recognized that some comets exhibit mid-IR spectral features attributable to crystalline silicates, typically crystalline olivine. The identification of Mg-rich crystalline olivine at 11.2 μm is secured by the *ISO* SWS spectrum of comet Hale-Bopp that shows the distinct longer wavelength features (Crovisier et al., 2000). On the other hand, some OC comets do not exhibit crystalline silicate emission features, although how much of this dichotomy is due to observational uncertainties will not be known until an analysis of a large number of comets is presented. Crystalline silicates are found in such high abundances in some comets that the crystals cannot be relics from the interstellar medium, where the crystalline fraction is $\leq 2.2\%$ (Kemper et al., 2004, 2005). For example, the crystalline-to-amorphous sub-μm mass ratio in the coma of the OC comet Hale-Bopp was 1.5–3.7 (Harker et al., 2002, 2004a). Recent observations have shown that JFCs also have crystals in significant fractional abundances: ∼0.3 for Deep Impact-induced inner coma (3″) of 9P/Tempel (Harker et al., 2005, 2007; Sugita et al., 2005) and ∼0.8 for the Deep-Impact larger coma (10″ Lisse et al., 2006), ∼0.9 for 78P/Gehrels (Watanabe et al., 2005), and qualitatively described as less than in Hale-Bopp is 73P-B/Schwassmann-Wachmann and 73P-C/Schwassmann-Wachmann (Harker et al., 2006b; Sitko et al., 2006d).

Exactly what conditions led to the formation of crystalline silicates and their transport to the comet forming zone is not known, but the high Mg-content of crystalline silicates found in comets requires significant processing of proto-solar nebula amorphous silicates (see a review by Wooden et al., 2007). Based on a legacy of solar nebula condensation models developed to explain minerals in chondrules and chondrites, Mg-Fe amorphous silicates evaporated and re-condensed at ∼ 1450 K as extremely Mg-rich silicate crystals and separate Fe grains in what is thought to be a typical "dry" solar nebula (Krot et al., 2000; Weinbruch et al., 2000). In addition, annealing, the process of heating an amorphous grain enough to crystallize it, may have been an important process. Based on a wide variety of experiments designed to create amorphous silicates and anneal them into crystals at ∼1000 K (see a review by Wooden et al., 2005), Mg-rich amorphous silicates anneal to Mg-rich crystalline silicates, Fe-rich amorphous silicates anneal to Fe-rich crystalline silicates, and Mg-Fe amorphous silicates anneal to Fe-bearing crystalline silicates (Brownlee et al., 2005) but the Fe-content in the crystals begins low (0.1) and increases (to 0.2) as the crystallization completes (Murata et al., 2007). The annealing products and activation energies somewhat depend on how the amorphous silicate starting materials are made in the laboratory (see the review by Wooden et al., 2005; Murata et al., 2007). The major issue with annealing to create cometary crystals is that Mg-rich amorphous silicates are not seen in cometary interplanetary dust particles or chondritic materials, so there is no reservoir with which to anneal to Mg-rich crystals. Instead, annealing of Mg-Fe amorphous grains to form Mg-rich crystals must occur in a low oxygen fugacity gas (i.e., when water is depleted relative to molecular hydrogen) where Fe can be reduced (removed by interdiffusion) (Davoisne et al., 2006; Wooden et al., 2007).

The small number abundance of Fe-rich crystals in cometary materials can be explained either by annealing without Fe reduction (e.g., Brownlee et al., 2005) or by

late-time condensation from the gas phase in a wet nebula (H_2O/H_2 ≈100–1000 times enhanced over a 'dry' nebula; Palme and Fegley, 1990). Interpretation of *Stardust* samples of comet 81P/Wild, where Fe-rich crystalline silicates are found in small numbers (Zolensky et al., 2007) but where secondary aqueous alteration products (e.g., layer lattice silicates) are not found (Zolensky et al., 2006), the gas phase condensation of moderately Fe-enriched to Fe-rich silicates is a more consistent scenario than parent body aqueous alteration. Moreover, we suggest that the condensation of Fe-rich crystalline silicates from a hot, water-rich nebula at times late enough for 90% of the Mg to have condensed into solids (Palme and Fegley, 1990) may explain the presence of Fe-rich crystalline silicates in both comets and in some chondrites that otherwise do not show extensive signs of parent body aqueous alteration.

As discussed above, Fe-rich crystalline silicates can condense from the gas phase when the oxygen fugacity is high. In order to have both Mg-rich and Fe-rich crystalline condensates, the water content must be variable. Water variability could come from inward migration of icy planetesimals into the hot inner-zones of the PPD (Cuzzi and Zahnle, 2004). Therefore, the differences between the comets with Mg-rich crystals and comet 9P/Tempel with Fe-rich crystals may be a matter of the epoch of each comet's formation, and the efficiency of radial transport in and out of the comet forming zones. Studying the abundance of Fe-rich crystalline silicates in bodies that have not undergone internal aqueous alteration (i.e., comets) may aid our understanding of the transport of water from beyond the frost line into the inner solar nebula, and the subsequent enrichment of the outer solar system with condensates that formed in a water rich environment.

6. Summary

We reviewed ground-based and space-based mid-IR spectra of Jupiter-family comets taken over the past 25 years. These observations, including spectroscopy of 9P/Tempel during the *Deep Impact* encounter and early *Spitzer* results, allow us to draw some conclusions on the nature of dust in JFCs: that, 1) JFCs have weak silicate emission features, roughly 20–25% over the continuum, similar to the lowest values observed in Oort Cloud comets; 2) the weak silicate emission could be due to low silicate content relative to other grain species (i.e., amorphous carbon and FeS), or due to the preponderance of large, compact grains ($\gtrsim$ 1 μm); 3) three JFCs show evidence for crystalline silicates in their mid-IR spectra (four if we include the Centaur-like 29P/Schwassmann-Wachmann)—the existence of crystals, also found in OC comet spectra, indicate high temperature processes altered some dust in the proto-planetary disk; 4) JFC nuclei can have heterogeneous dust properties, the evidence for which is presented in studies of the *Deep Impact* encounter with comet 9P/Tempel; 5) the evidence for hydrated minerals in the coma of 9P/Tempel is perplexing when we consider that comet interiors (for $R \leq 10$ km) likely remained well below the melting point of water ice; and, 6) the crystalline silicate forming zones of the solar nebula may have had a variable water content (i.e., variable oxygen fugacity) , which could lead to the apparent dichotomy of comets: comets that predominantly consist of Mg-rich crystals (e.g., comet Hale-Bopp), and comets with significant amounts of Fe-rich crystals (comet 9P/Tempel).

We identify several opportunities with which we may improve our understanding of dust in JFCs: 1) increase the number of observed JFC mid-IR spectra; 2) continue to model the thermal emission spectra of JFCs in order to ascertain the nature of their weak silicate features; 3) continue to compare models of light scattered by comet dust with thermal emission models to significantly constrain the structure of dust grains; and 4) employ the remarkable capabilities of 8–10 m class telescopes and SOFIA to improve our understanding of the amount and mineralogy of silicate crystals in comets, especially their Mg and Fe contents. We hope to answer: Why do JFCs and some OC comets have weak silicate emission features? How common are Fe-rich silicates and hydrated minerals in JFCs? Is the typical JFC heterogeneous in dust composition, and does that heterogeneity arise from the primordial aggregation of planetesimals?

Acknowledgments

The authors gratefully acknowledge D. E. Harker for providing Fig. 1 and Gemini spectra of comet 9P/Tempel. We also thank H. Campins and Y. R. Feranández for reviewing an early version of the manuscript, and thank T. Ootsubo and an anonymous referee, whose comments improved this paper.

References

A'Hearn, M. F., Schleicher, D. G., Millis, R. L., Feldman, P. D., Thompson, D. T., 1984. Comet Bowell 1980b. Astronomical Journal 89, 579-591.

A'Hearn, M. F., Millis, R. L., Schleicher, D. G., Osip, D. J., Birch, P. V., 1995. The ensemble properties of comets: Results from narrowband photometry of 85 comets, 1976-1992. Icarus 118, 223-270.

A'Hearn, M. F., and 32 colleagues, 2005. Deep Impact: Excavating Comet Tempel 1. Science 310, 258-264.

A'Hearn, M. F., Combi, M. R., 2007. Deep Impact at Comet Tempel 1. Icarus 187, 1-3.

Alexander, C. M. O., Barber, D. J., Hutchison, R., 1989. The microstructure of Semarkona and Bishunpur. Geochimica et Cosmochimica Acta 53, 3045-3057.

Armstrong, J. T., Meeker, G. P., Huneke, J. C., Wasserburg, G. J., 1982. The Blue Angel. I - The mineralogy and petrogenesis of a hibonite inclusion from the Murchison meteorite. Geochimica et Cosmochimica Acta 46, 575-595.

Becklin, E. E., Tielens, A. G. G. M., Gehrz, R. D., Callis, H. H. S., 2007. Stratospheric Observatory for Infrared Astronomy (SOFIA). In: Strojnik-Scholl, M. (Ed.), Infrared Spaceborne Remote Sensing and Instrumentation XV. Proceedings of the SPIE 6678, 66780A.

Belton, M. J. S., and 14 colleagues, 2007. The internal structure of Jupiter family cometary nuclei from Deep Impact observations: The "talps" or "layered pile" model. Icarus 191, 573-585.

Bockelée-Morvan, D., Crovisier, J., Mumma, M. J., Weaver, H. A., 2004. The composition of cometary volatiles. In: Festou, M. C., Keller, H. U., Weaver, H. A. (Eds.), Comets II 391-423.

Bockelee-Morvan, D., Woodward, C. E., Kelley, M. S., 2007. Water, PAHs, And Carbonate Emission Features In Spitzer Spectra Of Comets C/2003 K4 (linear) And 9P/Tempel 1. AAS/Division for Planetary Sciences Meeting Abstracts 39, #48.06.

Bradley, J. P., Snow, T. P., Brownlee, D. E., Hanner, M. S., 1999. Mg-Rich Olivine and Pyroxene Grains in Primitive Meteoritic Materials: Comparison with Crystalline Silicate Data from ISO. In: d'Hendecourt, L., Joblin, C., Jones, A. (Eds.), Solid Interstellar Matter: The ISO Revolution, Les Houches Workshop, February 2-6, 1998. EDP Sciences and Springer-Verlag.

Brearley, A. J., 2006. The Action of Water. Meteorites and the Early Solar System II 584-624.

Brownlee, D. E., 1985. Cosmic dust - Collection and research. Annual Review of Earth and Planetary Sciences 13, 147-173.

Brownlee, D. E., and 11 colleagues, 2004. Surface of Young Jupiter Family Comet 81 P/Wild 2: View from the Stardust Spacecraft. Science 304, 1764-1769.

Brownlee, D. E., Joswiak, D. J., Bradley, J. P., Matrajt, G., Wooden, D. H., 2005. Cooked GEMS – Insights into the Hot Origins of Crystalline Silicates in Circumstellar Disks and the Cold Origins of GEMS. 36th Annual Lunar and Planetary Science Conference 36, 2391.

Brownlee, D., and 182 colleagues, 2006. Comet 81P/Wild 2 Under a Microscope. Science 314, 1711.

Buratti, B. J., Hicks, M. D., Soderblom, L. A., Britt, D., Oberst, J., Hillier, J. K., 2004. Deep Space 1 photometry of the nucleus of Comet 19P/Borrelly. Icarus 167, 16-29.

Campins, H., Ryan, E. V., 1989. The identification of crystalline olivine in cometary silicates. Astrophysical Journal 341, 1059-1066.

Campins, H., Rieke, G. H., Lebofsky, M. J., 1982. Infrared photometry of periodic comets Encke, Chernykh, Kearns-Kwee, Stephan-Oterma, and Tuttle. Icarus 51, 461-465.

Carusi, A., Kresak, L., Perozzi, E., Valsecchi, G. B., 1985. Long-term evolution of short-period comets. Bristol: Hilger

Chihara, H., Koike, C., Tsuchiyama, A., 2001. Low-Temperature Optical Properties of Silicate Particles in the Far-Infrared Region. Publications of the Astronomical Society of Japan 53, 243-250.

Ciesla, F. J., Lauretta, D. S., Cohen, B. A., Hood, L. L., 2003. A Nebular Origin for Chondritic Fine-Grained Phyllosilicates. Science 299, 549-552.

Ciesla, F. J., 2007. Outward Transport of High-Temperature Materials Around the Midplane of the Solar Nebula. Science 318, 613.

Colangeli, L., Epifani, E., Brucato, J. R., Bussoletti, E., de Sanctis, C., Fulle, M., Mennella, V., Palomba, E., Palumbo, P., Rotundi, A., 1999. Infrared spectral observations of comet 103P/Hartley 2 by ISOPHOT. Astronomy and Astrophysics 343, L87-L90.

Crovisier, J., and 13 colleagues, 2000. The Thermal Infrared Spectra of Comets Hale-Bopp and 103P/Hartley 2 Observed with the Infrared Space Observatory. In: Sitko, M. L., Sprague, A. L., Lynch, D. K. (Eds.), Thermal Emission Spectroscopy and Analysis of Dust, Disks, and Regoliths. ASP Conf. Ser. 196, 109-117.

Crovisier, J., 2007. Cometary diversity and cometary families. Proceedings of the XVIIIemes Rencontres de Blois: Planetary Science: Challenges and Discoveries. (astro-ph/0703785).

Cuzzi, J. N., Zahnle, K. J., 2004. Material Enhancement in Protoplanetary Nebulae by Particle Drift through Evaporation Fronts. Astrophysical Journal 614, 490-496.

Davoisne, C., Djouadi, Z., Leroux, H., D'Hendecourt, L., Jones, A., Deboffle, D., 2006. The origin of GEMS in IDPs as deduced from microstructural evolution of amorphous silicates with annealing. Astronomy and Astrophysics 448, L1-L4.

Dorschner, J., Begemann, B., Henning, T., Jaeger, C., Mutschke, H., 1995. Steps toward interstellar silicate mineralogy. II. Study of Mg-Fe-silicate glasses of variable composition. Astronomy and Astrophysics 300, 503.

Duncan, M., Levison, H., Dones, L., 2004. Dynamical evolution of ecliptic comets. In: Festou, M. C., Keller, H. U., Weaver, H. A. (Eds.), Comets II 193-204.

Ehrenfreund, P., Charnley, S. B., Wooden, D., 2004. From interstellar material to comet particles and molecules. In: Festou, M. C., Keller, H. U., Weaver, H. A. (Eds.), Comets II 115-133.

Farnham, T. L., and 11 colleagues, 2007. Dust coma morphology in the Deep Impact images of Comet 9P/Tempel 1. Icarus 187, 26-40.

Feaga, L. M., A'Hearn, M. F., Sunshine, J. M., Groussin, O., Farnham, T. L., 2007. Asymmetries in the distribution of H_2O and CO_2 in the inner coma of Comet 9P/Tempel 1 as observed by Deep Impact. Icarus 190, 345-356.

Fegley, B. J., Prinn, R. G., 1989. Solar nebula chemistry - Implications for volatiles in the solar system. In: Weaver, H., Danly, L. (Eds.), The Formation and Evolution of Planetary Systems 171-205.

Fernández, Y. R., Lisse, C. M., Ulrich Käufl, H., Peschke, S. B., Weaver, H. A., A'Hearn, M. F., Lamy, P. P., Livengood, T. A., Kostiuk, T. 2000. Physical Properties of the Nucleus of Comet 2P/Encke. Icarus 147, 145-160.

Fernández, Y. R., Campins, H., Kassis, M., Hergenrother,

C. W., Binzel, R. P., Licandro, J., Hora, J. L., Adams, J. D., 2006. Comet 162P/Siding Spring: A Surprisingly Large Nucleus. Astronomical Journal 132, 1354-1360.

Gehrz, R. D., Ney, E. P., 1992. 0.7- to 23-micron photometric observations of P/Halley 2986 III and six recent bright comets. Icarus 100, 162-186.

Gehrz, R. D., Roellig, T. L., Werner, M. W., Fazio, G. G., Houck, J. R., Low, F. J., Rieke, G. H., Soifer, B. T., Levine, D. A., Romana, E. A., 2007. The NASA Spitzer Space Telescope. Review of Scientific Instruments 78, 1302.

Groussin, O., Lamy, P., Jorda, L., Toth, I., 2004. The nuclei of comets 126P/IRAS and 103P/Hartley 2. Astronomy and Astrophysics 419, 375-383.

Groussin, O., A'Hearn, M. F., Li, J.-Y., Thomas, P. C., Sunshine, J. M., Lisse, C. M., Meech, K. J., Farnham, T. L., Feaga, L. M., Delamere, W. A., 2007. Surface temperature of the nucleus of Comet 9P/Tempel 1. Icarus 191, 63-72.

Hage, J. I., Greenberg, J. M., 1990. A model for the optical properties of porous grains. Astrophysical Journal 361, 251-259.

Honda, M., and 13 colleagues, 2004. The 10 Micron Spectra of Comet C/2002 V1 (NEAT) and C/2001 RX14 (LINEAR). Astrophysical Journal 601, 577-582.

Hanner, M. S., Newburn, R. L., 1989. Infrared photometry of comet Wilson (1986l) at two epochs. Astronomical Journal 97, 254-261.

Hanner, M., Aitken, D., Roche, P., Whitmore, B., 1984. A search for the 10-micron silicate feature in periodic Comet Grigg-Skjellerup. Astronomical Journal 89, 170.

Hanner, M. S., Tedesco, E., Tokunaga, A. T., Veeder, G. J., Lester, D. F., Witteborn, F. C., Bregman, J. D., Gradie, J., Lebofsky, L., 1985. The dust coma of periodic Comet Churyumov-Gerasimenko (1982 VIII). Icarus 64, 11-19.

Hanner, M. S., Lynch, D. K., Russell, R. W., 1994. The 8-13 micron spectra of comets and the composition of silicate grains. Astrophysical Journal 425, 274-285.

Hanner, M. S., Lynch, D. K., Russell, R. W., Hackwell, J. A., Kellogg, R., Blaney, D., 1996., Mid-Infrared Spectra of Comets P/Borrelly, P/Faye, and P/Schaumasse. Icarus 124, 344-351.

Harker, D. E., Woodward, C. E., Wooden, D. H., Witteborn, F. C., Meyer, A. W., 1999. The 10 Micron Silicate Feature of Comet C/1996 Q1 (Tabur). Astronomical Journal 118, 1423-1429.

Harker, D. E., 1999. Silicate mineralogy of C/1995 O1 (Hale-Bopp) and its implications to the study of pre-main sequence stars and the origins of solar systems. Ph.D. Thesis. University of Wyoming.

Harker, D. E., Wooden, D. H., Woodward, C. E., Lisse, C. M., 2002. Grain Properties of Comet C/1995 O1 (Hale-Bopp). Astrophysical Journal 580, 579-597.

Harker, D. E., Wooden, D. H., Woodward, C. E., Lisse, C. M., 2004a. Erratum: "Grain Properties of Comet C/1995 O1 (Hale-Bopp)" (ApJ, 580, 579 [2002]). Astrophysical Journal 615, 1081-1081.

Harker, D. E., Woodward, C. E., Wooden, D. H., Kelley, M. S., 2004b. The Dust Mineralogy of Two Long-Period Comets: C/2001 Q4 (NEAT) and C/2002 T7 (LINEAR). Bulletin of the American Astronomical Society 36, 1434.

Harker, D. E., Woodward, C. E., Wooden, D. H., 2005. The Dust Grains from 9P/Tempel 1 Before and After the Encounter with Deep Impact. Science 310, 278-280.

Harker, D. E., Woodward, C. E., Sitko, M. L., Wooden, D. H., Lynch, D. K., Russell, R. W., 2006a. Comet 73P/Schwassmann-Wachmann. International Astronomical Union Circular 8708, 2.

Harker, D. E., Woodward, C. E., Sitko, M. L., Wooden, D. H., Russell, R. W., Lynch, D. K., 2006b. Mid-IR Gemini-N Observations Of Fragments B and C of Comet 73P/Schwassmann-Wachmann 3. Bulletin of the American Astronomical Society 38, 503.

Harker, D. E., Woodward, C. E., Wooden, D. H., Fisher, R. S., Trujillo, C. A., 2007. Gemini-N mid-IR observations of the dust properties of the ejecta excavated from Comet 9P/Tempel 1 during Deep Impact. Icarus 190, 432-453.

Harris, A. W., 1998. A Thermal Model for Near-Earth Asteroids. Icarus 131, 291-301.

Houck, J. R., and 34 colleagues, 2004. The Infrared Spectrograph (IRS) on the Spitzer Space Telescope. Astrophysical Journal Supplement Series 154, 18-24.

Jessberger, E. K., Christoforidis, A., Kissel, J., 1988. Aspects of the major element composition of Halley's dust. Nature 332, 691-695.

Jessberger, E. K., 1999. Rocky Cometary Particulates: Their Elemental, Isotopic and Mineralogical Ingredients. Space Science Reviews 90, 91-97.

Jewitt, D. C., 2002. From Kuiper Belt Object to Cometary Nucleus: The Missing Ultrared Matter. Astronomical Journal 123, 1039-1049.

Jewitt, D., 2004. Looking through the HIPPO: Nucleus and Dust in Comet 2P/Encke. Astronomical Journal 128, 3061-3069.

Jockers, K., Kiselev, N., Bonev, T., Rosenbush, V., Shakhovskoy, N., Kolesnikov, S., Efimov, Y., Shakhovskoy, D., Antonyuk, K., 2005. CCD imaging and aperture polarimetry of comet 2P/Encke: are there two polarimetric classes of comets? Astronomy and Astrophysics 441, 773-782.

Kadono, T., Sugita, S., Sako, S., Ootsubo, T., Honda, M., Kawakita, H., Miyata, T., Furusho, R., Watanabe, J., 2007. The Thickness and Formation Age of the Surface Layer on Comet 9P/Tempel 1. Astrophysical Journal 661, L89-L92.

Kelley, M. S., 2006. The size, structure, and mineralogy of comet dust. Ph.D. Thesis. University of Minnesota, Minneapolis, MN.

Kelley, M. S., and 10 colleagues, 2006. A Spitzer Study of Comets 2P/Encke, 67P/Churyumov-Gerasimenko, and C/2001 HT50 (LINEAR-NEAT). Astrophysical Journal 651, 1256-1271.

Keller, C., Gail, H.-P., 2004. Radial mixing in protoplan-

etary accretion disks. VI. Mixing by large-scale radial flows. Astronomy and Astrophysics 415, 1177-1185.

Keller, H. U., and 38 colleagues, 2007. Observations of Comet 9P/Tempel 1 around the Deep Impact event by the OSIRIS cameras onboard Rosetta. Icarus 191, 241-257.

Kemper, F., Vriend, W. J., Tielens, A. G. G. M., 2004. The Absence of Crystalline Silicates in the Diffuse Interstellar Medium. Astrophysical Journal 609, 826-837.

Kemper, F., Vriend, W. J., Tielens, A. G. G. M., 2005. Erratum: "The Absence of Crystalline Silicates in the Diffuse Interstellar Medium" (¡A href="/abs/2004ApJ...609..826K"¿ApJ, 609, 826 [2004]¡/A¿). Astrophysical Journal 633, 534-534.

Kimura, H., Kolokolova, L., Mann, I., 2003. Optical properties of cometary dust. Constraints from numerical studies on light scattering by aggregate particles. Astronomy and Astrophysics 407, L5-L8.

Kimura, H., Mann, I. 2004., Light scattering by large clusters of dipoles as an analog for cometary dust aggregates. Journal of Quantitative Spectroscopy and Radiative Transfer 89, 155-164.

Kimura, H., Kolokolova, L., Mann, I., 2006. Light scattering by cometary dust numerically simulated with aggregate particles consisting of identical spheres. Astronomy and Astrophysics 449, 1243-1254.

Kiselev, N. N., Jockers, K., Bonev, T. 2004. CCD imaging polarimetry of Comet 2P/Encke. Icarus 168, 385-391.

Koike, C., Chihara, H., Tsuchiyama, A., Suto, H., Sogawa, H., Okuda, H. 2003. Compositional dependence of infrared absorption spectra of crystalline silicate. II. Natural and synthetic olivines. Astronomy and Astrophysics 399, 1101-1107.

Kolokolova, L., Hanner, M. S., Levasseur-Regourd, A.-C., Gustafson, B. Å. S., 2004. Physical properties of cometary dust from light scattering and thermal emission. Comets II 577-604.

Kolokolova, L., Kimura, H., Kiselev, N., Rosenbush, V., 2007. Two different evolutionary types of comets proved by polarimetric and infrared properties of their dust. Astronomy and Astrophysics 463, 1189-1196.

Krot, A. N., Scott, E. R. D., Zolensky, M. E., 1995. Alteration and Dehydration in the Parent Asteroid of Allende. Meteoritics 30, 530-531.

Krot, A. N., Fegley, B., Jr., Lodders, K., Palme, H., 2000. Meteoritical and Astrophysical Constraints on the Oxidation State of the Solar Nebula. In: Mannings, V., Boss, A. P., Russell, S. S. (Eds.), Protostars and Planets IV, 1019.

Küppers, M., and 40 colleagues, 2005. A large dust/ice ratio in the nucleus of comet 9P/Tempel 1. Nature 437, 987-990.

Lagerros, J. S. V., 1998. Thermal physics of asteroids. IV. Thermal infrared beaming. Astronomy and Astrophysics 332, 1123-1132.

Lamy, P. L., Toth, I., Fernandez, Y. R., Weaver, H. A., 2004. The sizes, shapes, albedos, and colors of cometary nuclei. In: Festou, M. C., Keller, H. U., Weaver, H. A. (Eds.), Comets II 223-264.

Lebofsky, L. A., Sykes, M. V., Tedesco, E. F., Veeder, G. J., Matson, D. L., Brown, R. H., Gradie, J. C., Feierberg, M. A., Rudy, R. J., 1986. A refined 'standard' thermal model for asteroids based on observations of 1 Ceres and 2 Pallas. Icarus 68, 239-251.

Lewis, J. S., Barshay, S. S., Noyes, B. 1979. Primordial retention of carbon by the terrestrial planets. Icarus 37, 190-206.

Levasseur-Regourd, A. C., Hadamcik, E., Renard, J. B., 1996. Evidence for two classes of comets from their polarimetric properties at large phase angles.. Astronomy and Astrophysics 313, 327-333.

Levison, H. F., 1996. Comet Taxonomy. In: Rettig, T. W., Hahn, J. M. (Eds.), Completing the Inventory of the Solar System, ASP Conf. Ser. 107, 173-191.

Lisse, C. M., and 16 colleagues, 2006. Spitzer Spectral Observations of the Deep Impact Ejecta. Science 313, 635-640.

Lisse, C. M., Kraemer, K. E., Nuth, J. A., Li, A., Joswiak, D., 2007. Comparison of the composition of the Tempel 1 ejecta to the dust in Comet C/Hale Bopp 1995 O1 and YSO HD 100546. Icarus 187, 69-86.

Lynch, D. K., Hackwell, J. A., Edelsohn, D., Lahuis, F., Roelfsema, P. R., Wesselius, P. R., Walker, R. G., Sykes, M. V., 1995. IRAS LRS spectra of comets Tempel 1 and Tempel 2.. Icarus 114, 197-202.

Lynch, D. K., Russell, R. W., Sitko, M. 1998. Comets 55P/Tempel-Tuttle, 103P/Hartley 2, 69P/Taylor. International Astronomical Union Circular 6828, 3.

McKinnon, W. B., Prialnik, D., Stern, S. A., Coradini, A., 2008. Structure and Evolution of Kuiper Belt Objects and Dwarf Planets. The Solar System Beyond Neptune 213-241.

Meakin, P., Donn, B. 1988. Aerodynamic properties of fractal grains - Implications for the primordial solar nebula. Astrophysical Journal 329, L39-L41.

Merk, R., Prialnik, D., 2006. Combined modeling of thermal evolution and accretion of trans-neptunian objects–Occurrence of high temperatures and liquid water. Icarus 183, 283-295.

Meech, K. J., Svoreň, J., 2004. Using cometary activity to trace the physical and chemical evolution of cometary nuclei. In: Festou, M. C., Keller, H. U., Weaver, H. A. (Eds.), Comets II 317-335.

Min, M., Hovenier, J. W., de Koter, A., Waters, L. B. F. M., Dominik, C., 2005. The composition and size distribution of the dust in the coma of Comet Hale Bopp. Icarus 179, 158-173.

Min, M., Dominik, C., Hovenier, J. W., de Koter, A., Waters, L. B. F. M. 2006. The 10 boldsymbolμm amorphous silicate feature of fractal aggregates and compact particles with complex shapes. Astronomy and Astrophysics 445, 1005-1014.

Mukai, T., Ishimoto, H., Kozasa, T., Blum, J., Greenberg, J. M., 1992. Radiation pressure forces of fluffy porous

grains. Astronomy and Astrophysics 262, 315-320.

Mumma, M. J., DiSanti, M. A., Dello Russo, N., Magee-Sauer, K., Rettig, T. W., 2000. Detection of CO and Ethane in Comet 21P/Giacobini-Zinner: Evidence for Variable Chemistry in the Outer Solar Nebula. Astrophysical Journal 531, L155-L159.

Mumma, M. J., Disanti, M. A., dello Russo, N., Magee-Sauer, K., Gibb, E., Novak, R., 2003. Remote infrared observations of parent volatiles in comets: A window on the early solar system. Advances in Space Research 31, 2563-2575.

Moreno, F., Muñoz, O., Vilaplana, R., Molina, A., 2003. Irregular Particles in Comet C/1995 O1 Hale-Bopp Inferred from its Mid-Infrared Spectrum. Astrophysical Journal 595, 522-530.

Murata, K., Chihara, H., Tsuchiyama, A., Koike, C., Takakura, T., Noguchi, T., Nakamura, T., 2007. Crystallization Experiments on Amorphous Silicates with Chondritic Composition: Quantitative Formulation of the Crystallization. Astrophysical Journal 668, 285-293.

Nakamura, R., Kitada, Y., Mukai, T. 1994. Gas drag forces on fractal aggregates. Planetary and Space Science 42, 721-726.

Ootsubo, T., Watanabe, J.-I., Kawakita, H., Honda, M., Furusho, R., 2007a. Grain properties of Oort cloud comets: Modeling the mineralogical composition of cometary dust from mid-infrared emission features. Planetary and Space Science 55, 1044-1049.

Ootsubo, T., Sugita, S., Kadono, T., Honda, M., Sakon, I., Kawakita, H., Watanabe, J.-I., Subaru/Comics Team, 2007b. Mid-Infrared Observation of the Dust Plume from Comet 9P/Tempel 1 Generated by the Deep Impact Collision Using Subaru/Comics. Dust in Planetary Systems 643, 45-49.

Palme, H., Fegley, B. J., 1990. High-temperature condensation of iron-rich olivine in the solar nebula. Earth and Planetary Science Letters 101, 180-195.

Pittichova, J., Woodward, C. E., Kelley, M. S., Reach, W. T., 2008. Ground-based Optical and Spitzer Infrared Imaging Observations of Comet 21P/Giacobini-Zinner. Astronomical Journal, 136, 1127

Prialnik, D., Podolak, M., 1995. Radioactive heating of porous comet nuclei. Icarus 117, 420-430.

Prialnik, D., Podolak, M., 1999. Changes in the Structure of Comet Nuclei Due to Radioactive Heating. Space Science Reviews 90, 169-178.

Prialnik, D., Sarid, G., Rosenberg, E. D., Merk, R., 2008. Thermal and Chemical Evolution of Comet Nuclei and Kuiper Belt Objects. Space Science Reviews, in press (DOI: 10.1007/s11214-007-9301-4)

Schultz, P. H., Eberhardy, C. A., Ernst, C. M., A'Hearn, M. F., Sunshine, J. M., Lisse, C. M., 2007. The Deep Impact oblique impact cratering experiment. Icarus 191, 84-122.

Scott, E. R. D., Krot, A. N., 2005. Thermal Processing of Silicate Dust in the Solar Nebula: Clues from Primitive Chondrite Matrices. Astrophysical Journal 623, 571-578.

Sitko, M. L., Lynch, D. K., Russell, R. W., Hanner, M. S., 2004. 3-14 Micron Spectroscopy of Comets C/2002 O4 (Hönig), C/2002 V1 (NEAT), C/2002 X5 (Kudo-Fujikawa), C/2002 Y1 (Juels-Holvorcem), and 69P/Taylor and the Relationships among Grain Temperature, Silicate Band Strength, and Structure among Comet Families. Astrophysical Journal 612, 576-587.

Sitko, M. L., Russell, R. W., Lynch, D. K., Ford, R., Crawford, K., Polomski, E. F., Golisch, W., Griep, D., Sears, P., 2006a. Comet 73P/Schwassmann-Wachmann. International Astronomical Union Circular 8717, 1.

Sitko, M. L., Russell, R. W., Lynch, D. K., Ford, R., Hammel, H. B., Golisch, W., Sears, P., 2006b., Comet 73P/Schwassmann-Wachmann. International Astronomical Union Circular 8742, 2.

Sitko, M. L., Whitney, B. A., Wolff, M. J., Lisse, C. M., Polomski, E. F., Russell, R. W., Lynch, D. K., Harker, D. E., 2006d. Comet 73P/Schwassmann-Wachmann. International Astronomical Union Circular 8701, 3.

Stansberry, J. A., and 17 colleagues, 2004. Spitzer Observations of the Dust Coma and Nucleus of 29P/Schwassmann-Wachmann 1. Astrophysical Journal Supplement Series 154, 463-468.

Sugita, S., and 22 colleagues, 2005. Subaru Telescope Observations of Deep Impact. Science 310, 274-278.

Tancredi, G., Fernández, J. A., Rickman, H., Licandro, J., 2006. Nuclear magnitudes and the size distribution of Jupiter family comets. Icarus 182, 527-549.

Telesco, C. M., Decher, R., Baugher, C., Campins, H., Mozurkewich, D., Thronson, H. A., Cruikshank, D. P., Hammel, H. B., Larson, S., Sekanina, Z., 1986. Thermal-infrared and visual imaging of comet Giacobini-Zinner. Astrophysical Journal 310, L61-L65.

Tscharnuter, W. M., Gail, H.-P., 2007. 2-D preplanetary accretion disks. I. Hydrodynamics, chemistry, and mixing processes. Astronomy and Astrophysics 463, 369-392.

Voshchinnikov, N. V., Henning, T. 2008. Is the silicate emission feature only influenced by grain size?. Astronomy and Astrophysics 483, L9-L12.

Watanabe, J., Kawakita, H., Honda, M. Ootsubo, T., Fuse, T., Yamashita, T., Furusho, R., Kasuga, T., 2005. International Astronomical Union Symposium Abstracts 229, 121.

Weaver, H. A., Chin, G., Bockelée-Morvan, D., Crovisier, J., Brooke, T. Y., Cruikshank, D. P., Geballe, T. R., Kim, S. J., Meier, R. 1999. An Infrared Investigation of Volatiles in Comet 21P/Giacobini-Zinner. Icarus 142, 482-497.

Wehrstedt, M., 2003. 2-dimensional transport of tracers in protoplanetary accretion disks. Ph.D. Thesis, Naturwissenschaftlich-Mathematische Gesamtfakultät der Universität Heidelberg, Germany.

Wehrstedt, M., Gail, H.-P., 2003. Radial mixing in protoplanetary accretion disks. V. Models with different element mixtures. Astronomy and Astrophysics 410, 917-935.

Wehrstedt, M., Gail, H.-P., 2008. Radial mixing in proto-

planetary accretion disks VII. 2-dimensional transport of tracers. Astronomy and Astrophysics, submitted (astro-ph/0804.3377).

Weinbruch, S., Palme, H., Spettel, B., 2000. Refractory forsterite in primitive meteorites: condensates from the solar nebula? Meteoritics and Planetary Science 35, 161-171.

Werner, M. W., and 25 colleagues, 2004. The Spitzer Space Telescope Mission. Astrophysical Journal Supplement Series 154, 1-9.

Williams, D. M., Mason, C. G., Gehrz, R. D., Jones, T. J., Woodward, C. E., Harker, D. E., Hanner, M. S., Wooden, D. H., Witteborn, F. C., Butner, H. M., 1997. Measurement of Submicron Grains in the Coma of Comet Hale-Bopp C/1995 01 during 1997 February 15–20 UT. Astrophysical Journal 489, L91.

Wooden, D. H., Harker, D. E., Woodward, C. E., Butner, H. M., Koike, C., Witteborn, F. C., McMurtry, C. W., 1999. Silicate Mineralogy of the Dust in the Inner Coma of Comet C/1995 01 (Hale-Bopp) Pre- and Postperihelion. Astrophysical Journal 517, 1034-1058.

Wooden, D. H., 2002. Comet Grains: Their IR Emission and Their Relation to ISM Grains. Earth Moon and Planets 89, 247-287.

Wooden, D. H., Woodward, C. E., Harker, D. E., 2004. Discovery of Crystalline Silicates in Comet C/2001 Q4 (NEAT). Astrophysical Journal 612, L77-L80.

Wooden, D. H., Harker, D. E., Brearley, A. J., 2005. Thermal Processing and Radial Mixing of Dust: Evidence from Comets and Primitive Chondrites. In: Krot, A. N., Scott, E. R. D., Reipurth, B. (Eds), Chondrites and the Protoplanetary Disk. ASP Conf. Ser. 341, 774.

Wooden, D., Desch, S., Harker, D., Gail, H.-P., Keller, L., 2007. Comet Grains and Implications for Heating and Radial Mixing in the Protoplanetary Disk. In: Reipurth, B., Jewitt, D., Keil, K. (Eds.), Protostars and Planets V 815-833.

Wooden, D., 2008. Cometary Refractory Grains: Interstellar and Nebular Sources. Space Science Reviews, in press.

Woodward, C. E., Kelley, M. S., Harker, D. E., Wooden, D. H., Schleicher, D. G., 2002. Bulletin of the American Astronomical Society 34, 16.14.

Woodward, C. E., Kelley, M. S., Bockelée-Morvan, D., Gehrz, R. D., 2007. Water in Comet C/2003 K4 (LINEAR) with Spitzer. Astrophysical Journal 671, 1065-1074.

Xing, Z., Hanner, M. S., 1997. Light scattering by aggregate particles.. Astronomy and Astrophysics 324, 805-820.

Yamamoto, T., 1985. Formation environment of cometary nuclei in the primordial solar nebula. Astronomy and Astrophysics 142, 31-36.

Zolensky, M. E., Browning, L., 1997. Aqueous Alteration: Nebular and Asteroidal. In: Zolensky, M. E., Krot, A. N., Scott., E. R. D. (Eds.), Workshop on Parent-Body and Nebular Modifications of Chondritic Materials, Summary of Technical Sessions. LPI Technical Report 97-02, Part 2, 1.

Zolensky, M. E., and 74 colleagues, 2006. Mineralogy and Petrology of Comet 81P/Wild 2 Nucleus Samples. Science 314, 1735.

Zolensky, M., and 18 colleagues, 2007. Wild-2 Déjà-Vu: Comparison of Wild-2 Particles to Chondrites and IDPs. Lunar and Planetary Institute Conference Abstracts 38, 1481.

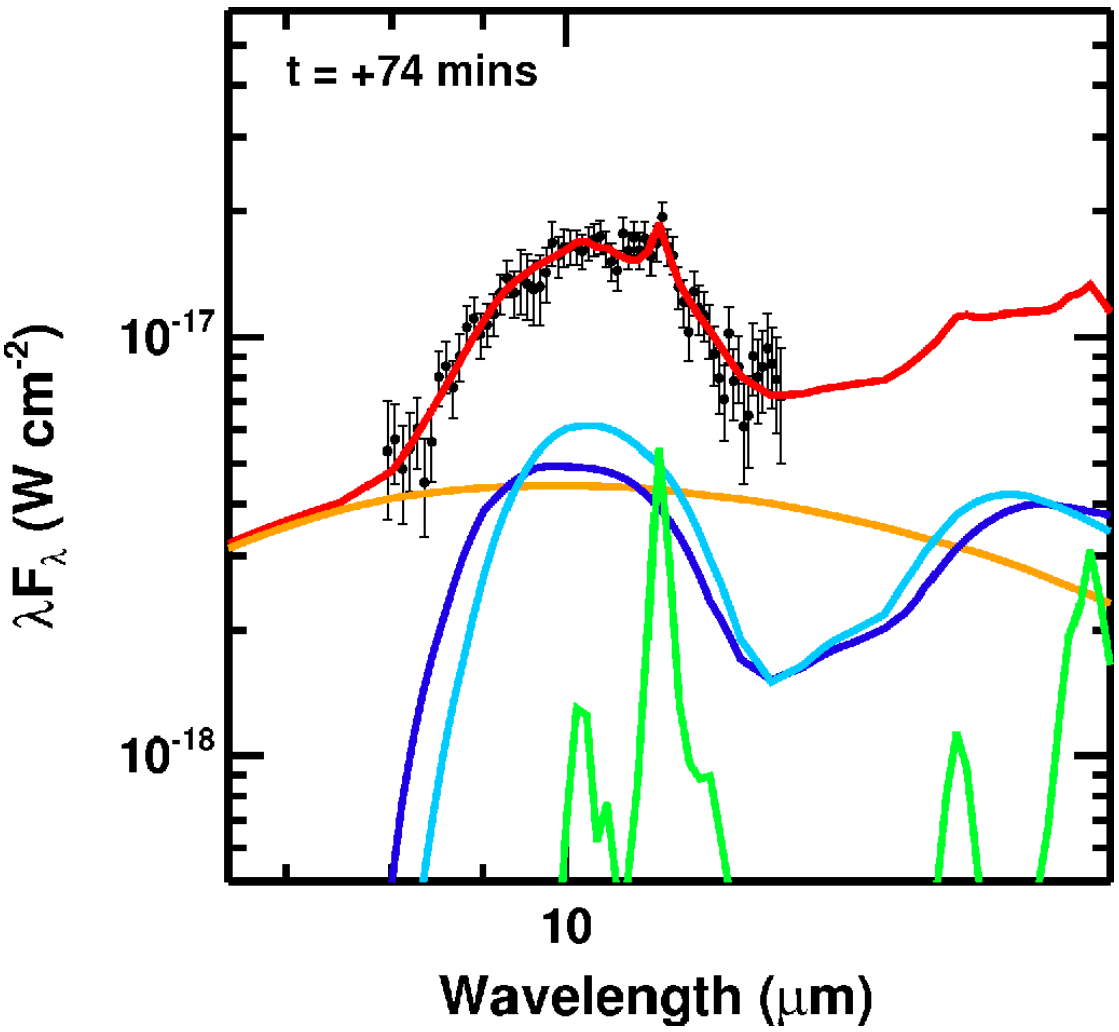

Fig. 1. Model spectra of the grain components detect in post-*Deep Impact* observations of 9P/Tempel from Harker et al. (2007). The Gemini-N/Michelle spectrum (*black circles*) is centered on the nucleus and is taken 74 min after impact. The thermal contribution of the nucleus is shown as an *orange line*. Superposed on the spectra is the total model spectral energy distribution (*red line*). The model is decomposed into its constituent dust components: amorphous pyroxene (*blue line*), amorphous olivine (*cyan line*), and crystalline olivine (*green line*). Notice the contrast between the broad spectral features of the amorphous silicates with the narrow resonances of crystalline olivine.

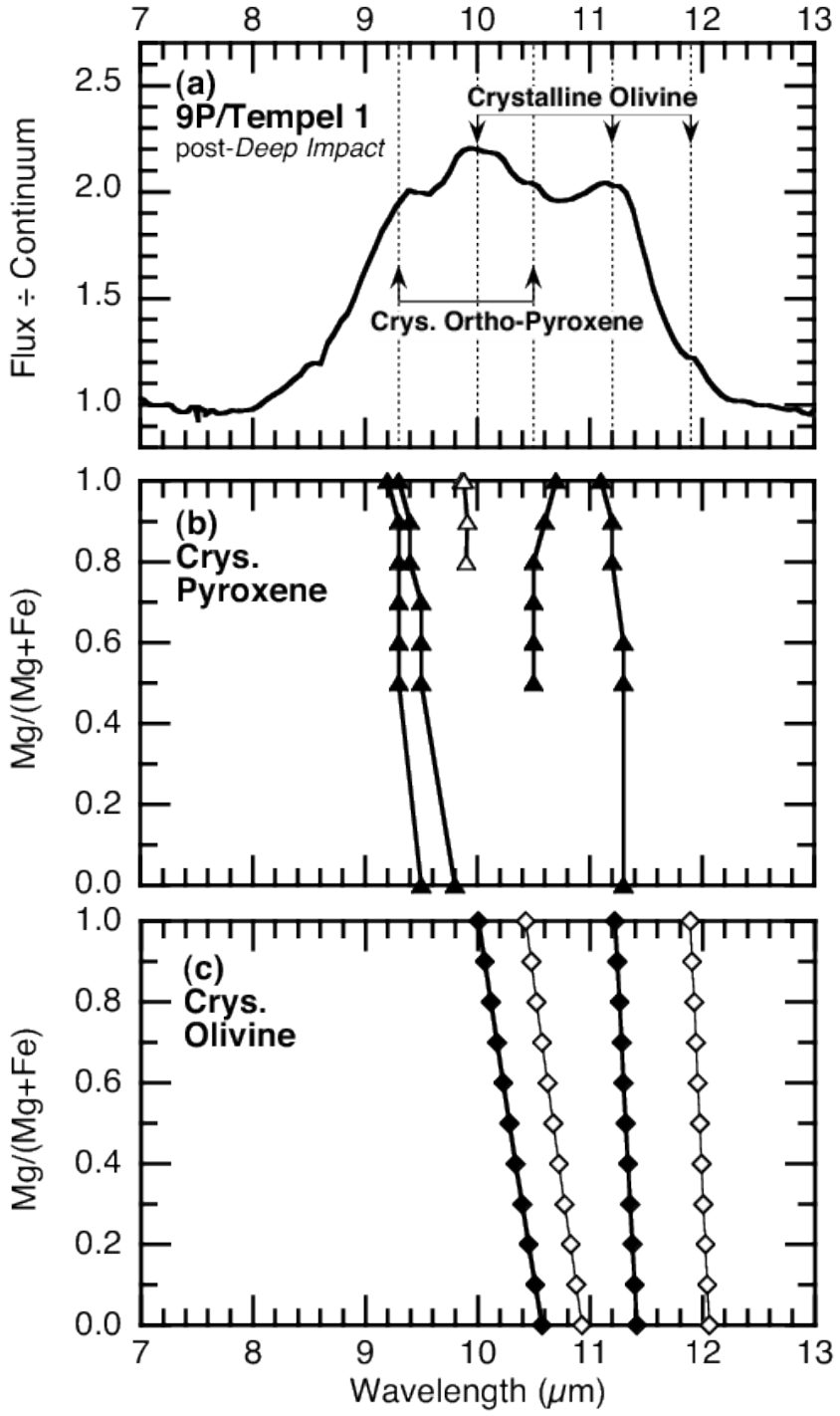

Fig. 2. The variation of selected resonance wavelength positions with Mg content in the 10 μm region for crystalline olivine (Koike et al., 2003) and crystalline ortho-pyroxene (Chihara et al., 2001). *Top*— A post-*Deep Impact Spitzer*/IRS spectrum of comet 9P/Tempel (1 hr after impact) normalized by a scaled Planck function fit to the spectrum at 8 and 12 μm (as described in §2). The wavelength positions for silicate crystalline peaks observed in comets C/1995 O1 (Hale-Bopp) (Wooden et al., 1999), C/2001 Q4 (NEAT) (Wooden et al., 2004), and 9P/Tempel (Harker et al., 2007) spectra are marked with *vertical dotted-lines*. *Center and Bottom*— *Filled symbols* mark the central wavelengths of strong silicate resonances as they vary with Mg content, *open symbols* mark weaker silicate resonances. The *y-axis* values range from 0.0 (Mg-poor, Fe-rich) to 1.0 (Mg-rich, Fe-poor) corresponding to the x and y parameters in each mineral's chemical composition: $[Mg_y,Fe_{1-y}]_2SiO_4$ (olivine) and $[Mg_x,Fe_{1-x}]SiO_3$ (pyroxene).

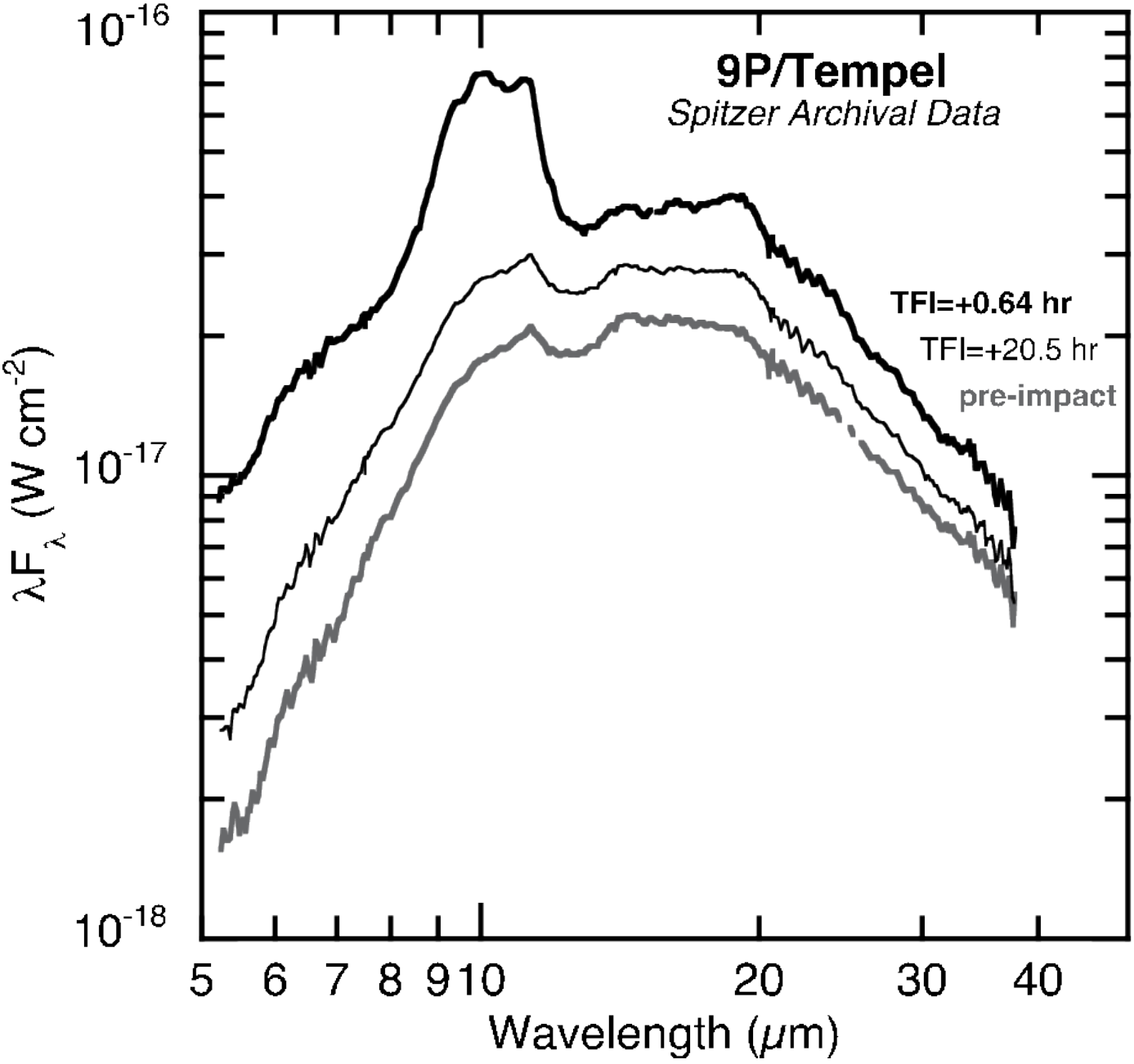

Fig. 3. Pre-impact spectrum of comet 9P/Tempel taken 03 July 2005 UT (*gray line*), and two spectra taken 0.64 (*thick black line*) and 20.5 hr (*thin black line*) after impact. The contribution from a 3.3 km nucleus has been removed. Notice the broad amorphous silicate emission at 8–12 and 15–20 μm in the pre-impact spectra. Also note the strong crystalline resonances at 9 and 11 μm in the first post-impact spectrum.

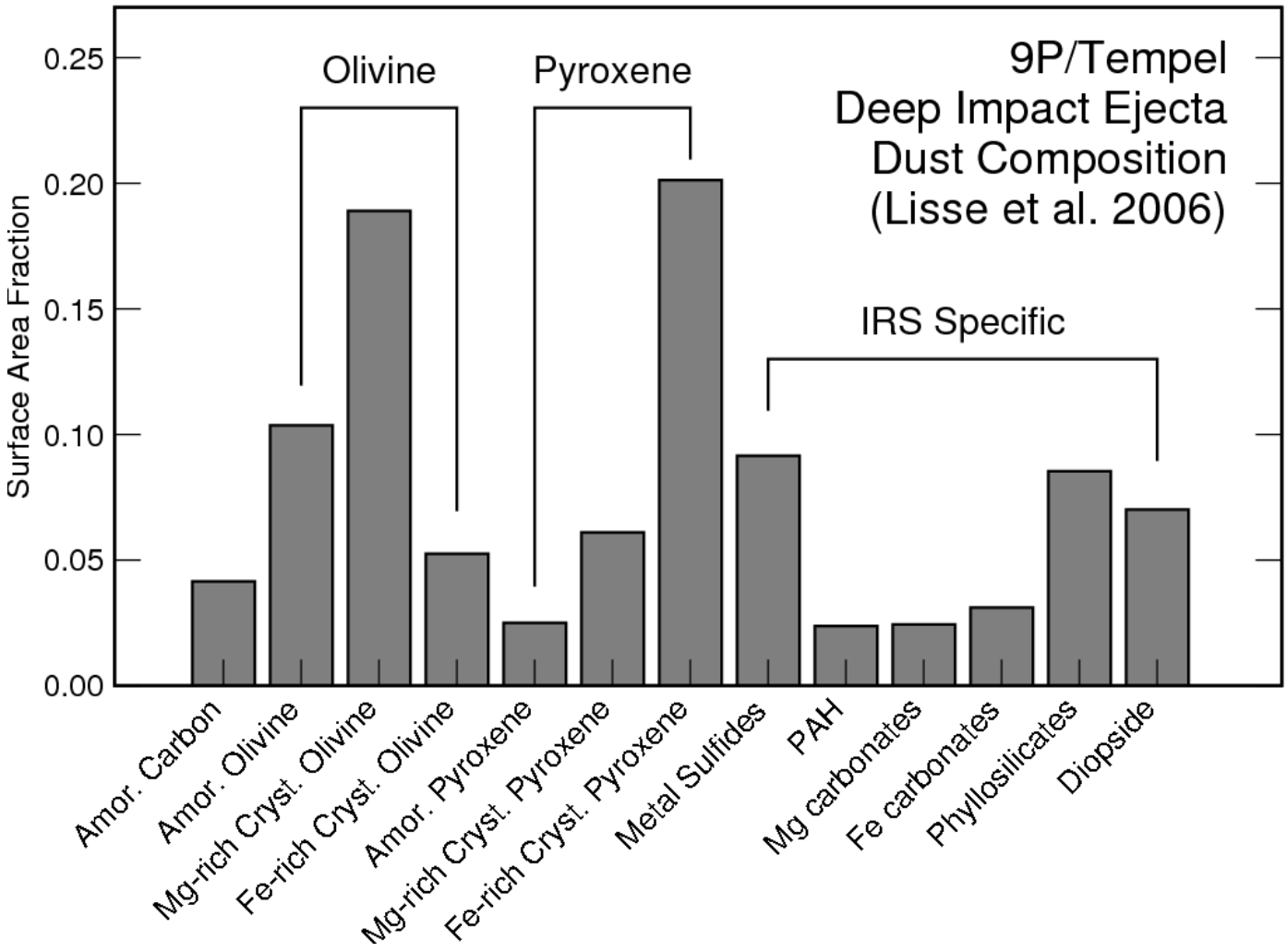

Fig. 4. Grain components identified in the mid-IR in post-*Deep Impact Spitzer* spectra of comet 9P/Tempel (Lisse et al., 2006). In order to emphasize the importance of space-based infrared spectra, we have highlighted those components that have only been identified through reduced χ^2 fits to the *Spitzer*/IRS 5–35 μm observations.

Table 1: Mid-infrared spectroscopy of Jupiter-family comets.

Comet	Investigators	Telescope	Instrument	10 μm Silicate Band Strength	Notes
2P/Encke	Kelley et al. 2006	*Spitzer*	IRS	N	Silicates are $< 31\%$ of the sub-μm dust mass (3σ).
4P/Faye	Hanner et al. 1996	IRTF	BASS	1.25	
9P/Tempel	Lynch et al. 1995	IRAS	LRS	< 1.40 [b]	
	Lisse et al. 2006	*Spitzer*	IRS	Y	We find the silicate band strength to be pre-*Deep Impact*: 1.19–1.25 (Fig. 3); 0.64 hr post-*Deep Impact*: 1.95–2.21
	Harker et al. 2007	Gemini-N	Michelle	Y	We find the silicate band strength to be pre-*Deep Impact*: May 2005 1.50 ± 0.18, July 2005 1.2 ± 0.2; 74 min post-*Deep Impact*: 2.02–2.16
	Ootsubo et al. 2007b	Subaru	COMICS	Y	
10P/Tempel	Lynch et al. 1995	IRAS	LRS	< 1.40 [b]	
19P/Borrelly	Hanner et al. 1996	IRTF	BASS	1.11 [b]	1.13–1.19 after nucleus subtraction.
	Woodward et al. 2002	IRTF	HIFOGS	N	
24P/Schaumasse	Hanner et al. 1996	IRTF	BASS	< 1.10 [b]	Bare nucleus?
26P/Grigg-Skjellerup	Hanner et al. 1984	UKIRT	UCL Spec.	N	
29P/Schwassmann-Wachmann [a]	Stansberry et al. 2004	*Spitzer*	IRS	1.10 [b]	1.19 after nucleus subtraction.
67P/Churyumov-Gerasimenko	Hanner et al. 1985	IRTF	FOGS	N	
	Kelley et al. 2006	*Spitzer*	IRS	...	
69P/Taylor	Sitko et al. 2004	IRTF	BASS	1.23 [b]	1.24–1.28 after nucleus subtraction.
73P/Schwassmann-Wachmann	Harker et al. 2006a	Gemini-N	Michelle	1.15–1.25	Fragments B and C
	Sitko et al. 2006a,b	IRTF	BASS	1.18–1.25	Fragments B and C
	Sitko et al. 2006d	*Spitzer*	IRS	1.33	Fragment B
78P/Gehrels	Watanabe et al. 2005	Subaru	COMICS	Y	
103P/Hartley	Lynch et al. 1998	IRTF	BASS	1.15 [b]	1.22 after nucleus subtraction.
	Colangeli et al. 1999	ISO	ISOPHOT	N	The uncertainties may be consistent with ≤ 1.2
	Crovisier et al. 2000	ISO	ISOCAM	1.20 [b]	The nucleus is $\leq 1\%$ of the flux.

[a] The Tisserand parameter of 29P is $T_J = 2.98$, which places the comet in the Jupiter-family class (Levison, 1996), yet in long timescale integrations, the comet always remains between the orbits of Jupiter and Saturn (see, e.g., Carusi et al., 1985)—a behavior that is similar to Centaurs. Since Centaurs and Jupiter-family comets have the same origin in today's solar system (the Kuiper Belt and Scattered Disk) their dust properties are related, and a comparison between 29P and JFCs is valid.

[b] These silicate band strengths do not take into consideration the flux from the nucleus. For most entries, we list a corrected value in the notes column.

Table 2
Coma (F_C) and nucleus (F_N) fluxes at 10 μm for our "median Jupiter-family comet" model.[a]

Δ (AU)	Phase angle (°)	F_N (mJy)	F_C ($\theta = 0.20''$)[b] (mJy)	$0.8F_N/(0.8F_N + F_C)$ [c]		
				$\theta = 0.20''$	$\theta = 0.60''$	$\theta = 1.85''$
$Af\rho = 110$ cm, $r_h = 1.8$ AU, $R_n = 1.8$ km						
0.8	0	158	9	0.93	0.82	0.60
1.0	25	91	7	0.91	0.77	0.52
1.2	31	60	6	0.89	0.73	0.46
$Af\rho = 430$ cm[d], $r_h = 1.0$ AU, $R_n = 1.8$ km						
0.3	81	1602	481	0.73	0.47	0.22
0.6	72	488	240	0.62	0.35	0.15
0.9	63	259	160	0.56	0.30	0.12

[a] See §3.3 for a discussion of the model parameters. Note that F_C, F_N, and their ratio vary with wavelength.

[b] The coma flux scales linearly with aperture angular radius, θ, for constant isotropic dust ejection (Eq. 2).

[c] The aperture angular radius for the $R \approx 100$ mode of three instruments: $\theta = 0.20''$ corresponds to Gemini/Michelle, $\theta = 0.60''$ to IRTF/MIRSI, and $\theta = 1.85''$ to *Spitzer*/IRS. For simplicity, we assume a slit throughput of 80% for point sources (the nucleus).

[d] To estimate the $Af\rho$ at $r_h = 1.0$ AU, we scaled the $Af\rho$ at $r_h = 1.8$ AU by a factor of $1.8^{2.3}$ as suggested by A'Hearn et al. (1995).